

JGR Biogeosciences

RESEARCH ARTICLE

10.1029/2020JG005986

Key Points:

- Differing forest and woodland ecosystems show similarities in precipitation and soil moisture relationships that inform future functioning
- Timing of soil moisture defined seasons differs between high and low elevations, yet differences are reduced by low or high precipitation
- Shallow and deeper soil moisture are often physically disconnected, yet are shaped by low and high seasonal precipitation similarly

Correspondence to:

M. D. Petrie,
matthew.petrie@unlv.edu

Citation:

Koehn, C. R., Petrie, M. D., Bradford, J. B., Litvak, M. E., & Strachan, S. (2021). Seasonal precipitation and soil moisture relationships across forests and woodlands in the southwestern United States. *Journal of Geophysical Research: Biogeosciences*, 126, e2020JG005986. <https://doi.org/10.1029/2020JG005986>

Received 28 JUL 2020

Accepted 12 JAN 2021

Author Contributions:

Conceptualization: M. D. Petrie, J. B. Bradford, M. E. Litvak, S. Strachan

Data curation: C. R. Koehn, M. D. Petrie, J. B. Bradford, M. E. Litvak, S. Strachan

Formal analysis: C. R. Koehn, M. D. Petrie

Investigation: C. R. Koehn, M. D. Petrie

Methodology: C. R. Koehn, M. D. Petrie

Software: M. D. Petrie

Supervision: M. D. Petrie

Visualization: M. D. Petrie

Writing – original draft: C. R. Koehn, M. D. Petrie, J. B. Bradford, M. E. Litvak, S. Strachan

Writing – review & editing: M. D. Petrie

Seasonal Precipitation and Soil Moisture Relationships Across Forests and Woodlands in the Southwestern United States

C. R. Koehn¹ , M. D. Petrie¹ , J. B. Bradford², M. E. Litvak³ , and S. Strachan⁴ 

¹School of Life Sciences, University of Nevada, Las Vegas, Las Vegas, NV, USA, ²United States Geological Survey, Southwest Biological Science Center, Flagstaff, AZ, USA, ³Department of Biology, University of New Mexico, Albuquerque, NM, USA, ⁴Office of Information Technology, University of Nevada Reno, Reno, NV, USA

Abstract Precipitation [P: mm] controls forest and woodland dynamics in the southwestern United States (SWUS) by altering soil moisture [θ : mm³ mm⁻³] availability, but the influence of P on θ is complex, varying across space and time. We evaluated seasonal P and θ relationships at shallow (0–20 cm) and intermediate (50 cm) soil depths for nine semiarid forest and woodland sites (56 total years), which comprised three elevation gradients in the SWUS. We developed time-varying definitions of winter (snow accumulation), spring (moisture recharge), and summer (moisture deficit), and determined how these sites exhibited similar P influence on θ across depths in the soil profile, between seasons, and in seasons with above- and below-average P. Higher elevation sites (>2,800 m) experienced greater winter P, longer springs, and shorter summers compared to lower elevation sites (<2,500 m). Seasons with above- and below-average P reduced elevation-associated differences. θ at 0–20 cm was generally decoupled from θ at 50 cm in seasons with average and below-average P, imparted by differences in spring and summer rainfall versus winter snowfall. Notably, across-season influence of θ (e.g., a season's similarity to subsequent seasons) was high when the first season experienced above- or below-average P, and the subsequent season experienced average P, illustrating an important temporal connection initiated by wet and dry conditions. These results illustrate similarities in P- θ relationships across widely differing ecosystems in the SWUS, and elucidate how these relationships may be altered in a changing climate.

Plain Language Summary Soil moisture is an important and limiting resource for forests and woodlands in the southwestern US, and is controlled by precipitation patterns that differ widely across the region. We evaluated winter (snowfall, rainfall) and spring and summer (rainfall) relationships to soil moisture at shallow (0–20 cm) and intermediate (50 cm) soil depths at nine diverse forest and woodland sites in this region. Using a novel approach that defined winter, spring, and summer by their soil moisture patterns, we investigated how precipitation at these sites influenced soil moisture across soil depths, between seasons, and in seasons with high and low precipitation. Higher elevation sites had greater winter precipitation, longer springs, and shorter summers than lower elevation sites, but years with high or low precipitation reduced these differences. Across all sites, shallow soil moisture had little similarity to intermediate soil moisture, yet moisture at both shallow and intermediate soil depths could be strongly influenced by previous seasons with substantially lower or higher precipitation. Our study illustrates similarity in how precipitation influences soil moisture availability across diverse forest and woodland ecosystems in this region, and elucidates fundamental relationships that govern how they respond to seasonal variation in climate.

1. Introduction

In the southwestern United States (SWUS), coniferous forests and pinyon pine-juniper woodlands are prevalent across a broad range of environmental conditions and contribute considerably to ecosystem services throughout the region (Hartsell et al., 2020; Hurteau et al., 2014; Rocca et al., 2014). These ecosystems have experienced numerous disturbance events over the past 60 years that, when combined with the potential stresses of global climate change, makes their long-term persistence questionable in much of this region (Allen & Breshears, 1998; Kolb et al., 2013; Littell et al., 2009; A. P. Williams et al., 2010). Past declines in these ecosystems can be tied to widespread industrial exploitation in the mid to late 1800s (Young &

Budy, 1979) and more recently to extended periods of low precipitation [P : mm] and low soil moisture [θ : $\text{mm}^3 \text{mm}^{-3}$], such as during drought events in the 1950s and early 2000s that resulted in regional tree mortality (Allen & Breshears, 1998; Swetnam & Betancourt, 1998; A. P. Williams et al., 2013). Yet, regional forest and woodland responses were highly heterogeneous across the SWUS during these drought events, and in many cases cannot be attributed solely to decreased total P (Breshears et al., 2005). Similar to other semiarid ecosystems, the effects of P on θ in forests and woodlands of the SWUS are shaped by variation in local factors including elevation, microclimate, and physical soil properties (Breshears et al., 2005; Koepke et al., 2010). This regional and local heterogeneity in P - θ relationships, as well as historic disturbance and exploitation practices, complicates understanding of the ecological consequences of variable P regimes across the SWUS.

Climate change is expected to increase variability in seasonal P and alter seasonal patterns of θ availability (Allan & Soden, 2008; Bradford et al., 2020), which makes forecasting the consequences of climate change for forests and woodlands in the SWUS tenuous. Seasonal periods of both high and low P are predicted to become more frequent, and transitions between wet and dry conditions are expected to become more prominent (Allan & Soden, 2008; Demaria et al., 2019; Fischer & Knutti, 2016). Dry periods increase stress to trees by increasing the magnitude and duration of θ deficit, and climate change is predicted to intensify dry periods through increasing P variability, through temperature-driven increases in evapotranspiration and vapor pressure deficit, and by decreasing spring snowpack (Cayan et al., 2010; Seager & Vecchi, 2010; A. P. Williams et al., 2013). Thus, climate change is expected to intensify climate associated stressors that have already had significant impacts to these ecosystems.

In contrast to the deleterious climate impacts to forest and woodland ecosystems initiated by dry conditions, above-average P periods on the scale of multiple days to multiple years are beneficial for coniferous trees, may help forest and woodland ecosystems recover from past disturbance events, and may insulate them from subsequent dry periods (Brown & Wu, 2005; Swetnam & Betancourt, 1998). Similar to dry periods, the positive impacts of high P and associated θ surplus are also influenced by landscape heterogeneity (Dobrowski, 2011; Herrmann et al., 2016; Oldfather et al., 2016). Thus, the interplay between the effects of beneficial wet periods and deleterious dry periods varies by seasonal P patterns and landscape effects (Van Loon & Van Lanen, 2012; Van Loon et al., 2014), and understanding P - θ relationships across landscape diversity in the SWUS is a key component of understanding the current and future dynamics of forest and woodland ecosystems.

Variability in P forcings complicates understanding of the effects of climate patterns on forest and woodland ecosystems by imparting extreme variation in P totals that vary across both space and time. Regionally, interannual variation in the North American monsoon system is a large source of warm season precipitation in some areas of the SWUS, and is entirely absent from others (Adams & Comrie, 1997). Variation in the North American monsoon is often tied to both summer and winter P totals. Generally, winter P variability has greater effects on ecosystem θ dynamics in locations with large differences in winter and summer P totals, such as the northern areas of the SWUS that do not experience a strong summer monsoon (Van Loon et al., 2014). In more southerly SWUS locations with stronger monsoon rainfall, moisture availability and deficit is strongly tied to the occurrence of large rainfall events (Petrie et al., 2014; Van Loon & Van Lanen, 2012), and summer P totals may be more ecologically important for forests and woodlands that are adapted to respond to summer rainfall (Limousin et al., 2013). Moreover, variability in seasonal P totals and P event characteristics can both enhance and reduce the effects of both positive high P and deleterious low P in ways that are highly variable over multiyear time periods (Strachan, 2016; Swetnam & Betancourt, 1998). By understanding how seasonal P totals influence θ across more northerly and southerly SWUS locations, it may be possible to identify general patterns of P - θ relationships, and reduce some of the uncertainty surrounding regional P variability.

At local scales, variation in landscape conditions—especially elevation—imparts a strong control on P totals and θ availability. In the SWUS, elevation change is correlated to gradients in vegetation types and structure (Whittaker & Niering, 1965), air temperature (Anderson-Teixeira et al., 2011), snowpack magnitude and the timing of snowmelt (Hunsaker et al., 2012), and the magnitude of large-scale spring and summer P forcings (Zlotin & Parmenter, 2008). Local variation in aspect and elevation has been found to delay or advance snowmelt and dry season onset by up to 4 weeks (Bales et al., 2011). Aspect, slope, and soil texture are

factors that varies across elevation gradients as well as between individual sites that affect P infiltration into soil (Blankinship et al., 2014; C. J. Williams et al., 2009). Both regional P forcings and local P- θ interactions have great effects on magnitude and timing of θ availability.

Together, the effects of regional and local variation in climate and landscape factors influence where θ is stored in the soil profile. θ storage patterns in the soil profile are critically important for different components of forest and woodland ecosystems. For instance, in lower-elevation pinyon-juniper woodlands, pinyon pines are adapted to utilize θ at shallow soil depths (0–10 cm) that are more readily recharged by small rainfall events, whereas junipers (*Juniperus osteosperma*) may require events that penetrate to at least 20 cm (West et al., 2007). At higher elevations, θ at very shallow soil depths (0–10 cm) is important for ponderosa pine germination, but juvenile survival is tied to the ability of tree seedlings to access θ deeper in the soil profile (Petrie et al., 2017). Meanwhile, mature ponderosa pines (60+ years old) can acquire water from soil depths that may be as great as 1.5 m deep (Berndt & Gibbons, 1958) and primarily use deeper, winter-derived soil moisture (Kerhoulas et al., 2013). Shallow θ (0–10 cm) can receive moisture inputs from modest precipitation events, but may be rapidly evaporated (Newman et al., 1997). Conversely, deeper θ requires large moisture inputs, often in the form of spring snowmelt or uncommonly large summer rainfall events (Kerhoulas et al., 2013). A number of studies predict a future change to the P patterns that partition θ between shallow and deeper soil layers (see Bradford et al. [2020], Seager and Vecchi [2010], and Cayan et al. [2010] for examples). As a result, not only are regional climate patterns and local landscape patterns important for understanding the importance of P- θ relationships in forest and woodland ecosystems of the SWUS, it is important to know how these components shape the patterns of belowground θ that control the dynamics of these ecosystems.

Wide variation in climate and landscape conditions complicates biophysical understanding of forests and woodlands of the SWUS, yet there is opportunity to reduce this uncertainty by identifying similarities and differences in P- θ relationships that can be used to anticipate the ecological importance of P variability for these ecosystems. In this study, we determined similarities and differences in seasonal P- θ relationships for nine semiarid forest and woodland sites in the SWUS (56 years in total). These sites comprised three elevation gradients with a combined range of 1,930–3,355 m and exhibit notable differences in regional P forcings, yet all are considered semiarid ecosystems with mean annual P less than 600 mm. Our objectives were to: (a) identify broad similarities and differences in seasonal P- θ relationships across these sites, (b) evaluate how the influence of P (winter snowfall and rainfall, spring and summer rainfall) on θ dynamics changed across these sites in wet, average, and dry seasons, (c) determine how P- θ relationships change for θ in shallow (0–10 cm, 10–20 cm) versus intermediate (50 cm) depths in the soil profile, and (d) determine under what conditions early season θ (winter, spring) informs θ in later seasons (spring, summer). Our evaluation of P- θ relationships was based on a novel and relatively simple approach that identified the length and properties of winter, spring, and summer based on θ patterns at each individual site in each year. We hypothesized that all sites would display a similar pattern of θ recharge and depletion over yearly cycles, supporting the conclusion that θ trends at lower elevation sites can be used to anticipate a warmer climatic future at higher elevation sites with the influence of climate change. Our study provides insight on broad similarities and differences in P- θ relationships across forests and woodlands of the SWUS and identifies the P conditions that induce change to these relationships in ways that are likely to be ecologically meaningful.

2. Site Description

Our study included nine forest and woodland sites within three elevation gradients in the SWUS: The Snake Mountain Range in northeastern Nevada (NevCAN; <https://nevcan.dri.edu>), Valles Caldera in northern New Mexico (NMEG; <https://www.litvaklab.org/new-mexico-elevation-gradient.html>), and northern Arizona (SEGA; <https://sega.nau.edu/home>; Table 1, Figure 1). NevCAN sites included a mixed pine forest (Snake Range West Subalpine; NV-H), a white fir forest (Snake Range West Montane; NV-M), and a pinyon-juniper woodland (Snake Range Pinyon-Juniper; NV-L). NMEG sites included a mixed conifer forest before and after a stand replacing burn (Valles Caldera Mixed Conifer preburn; NM-Hp and Valles Caldera Mixed Conifer postburn; NM-Hb) and a ponderosa pine forest (Valles Caldera Ponderosa Pine; NM-M). SEGA sites included a mixed conifer forest (Camp Colton; AZ-H), a ponderosa pine forest and alpine meadow (Arboretum; AZ-M), and a pinyon-juniper woodland (Blue Chute; AZ-L). Abbreviations are designated

Table 1

Site Descriptions Including Coordinates, Elevation, Ecosystem Type, Mean Annual P, Percent Summer and Winter P, Years of Available Data, and Days of Missing θ Data

Name	Coordinates	Elevation (m)	Ecosystem	Mean air temperature (°C)	Mean annual P (mm)	Summer (JJA) P (%)	Winter (DJF) P (%)	Data range (years)	Days missing
NevCAN Snake Range West Subalpine (NV-H)	38.906114, -114.308911	3,355	Mixed pine forest	1.62 ± 8.33	490 ± 150	20	26	2013–2018	0
NevCAN Snake Range West Montane (NV-M)	38.889838, -114.331384	2,810	White fir forest	5.45 ± 8.93	400 ± 110	19	25	2012–2018	0
NevCAN Snake Range Pinyon-Juniper (NV-L)	38.892167, -114.350044	2,200	Pinyon-juniper woodland	9.68 ± 9.34	320 ± 70	21	27	2012–2018	0
NMEG Valles Caldera Mixed Conifer PreBurn (NM-Hp)	35.888447, -106.532114	3,030	Mixed conifer forest	4.38 ± 8.34	580 ± 250	32	24	2007–2010, 2012	125
NMEG Valles Caldera Mixed Conifer PostBurn (NM-Hb)	35.888447, -106.532114	3,030	Mixed conifer after stand replacing burn	5.07 ± 7.70	430 ± 60	47	7	2014–2018	0
NMEG Valles Caldera Ponderosa Pine (NM-M)	35.864231, -106.596664	2,500	Ponderosa pine forest	7.22 ± 8.13	430 ± 80	39	17	2008–2018	0
SEGA Camp Colton (AZ-H)	35.329, -111.73	2,591	Mixed conifer forest	7.41 ± 0.88	560 ± 80	49	14	2015–2019	50
SEGA Arboretum (AZ-M)	35.16, -111.73	2,200	Ponderosa pine forest and alpine meadow	7.12 ± 8.09	300 ± 40	38	19	2015–2019	76
SEGA Blue Chute (AZ-L)	35.58, -111.97	1,930	Pinyon-juniper woodland	11.23 ± 8.91	480 ± 100	37	26	2015–2018	134

Note. Means are given with ± 1 SD. Mean annual P was calculated using water year. Summer and winter P are given as the percentage of total recorded P occurring in those time periods. Data are not gap filled. Due to missing data, the Blue Chute P is determined from PRISM data (PRISM Climate Group at Oregon State University, 2004).

by location of the site gradient and the site's placement within that gradient (high, medium, or low); thus, an H at one location may be at a lower elevation than an M at another location. Collectively, these sites comprise a range of elevations from 1,930 (SEGA) to 3,355 m (NevCAN; Table 1) and cover a range of ecosystems from pinyon-juniper woodlands to mixed conifer forests. The locations for these sites encompass a relatively broad range of climates experienced by forests and woodlands in the SWUS. All sites are semiarid forests or woodlands (mean annual P less than 600 mm), but the SEGA and NMEG sites experience monsoon-driven summer rainfall, whereas the NevCAN sites experience proportionally lower summer rainfall (Table 1). During the time periods of our study, sites experienced wide variation in seasonal P totals, and many site-years exhibited above-average P in one season and below-average P in another (Table 2). Mean annual temperatures across all nine sites ranged from 1.62°C at the highest elevation site (NV-H) to 11.23°C at the lowest elevation site (AZ-L).

3. Methods

3.1. Data Sources and Processing

We obtained precipitation [P: mm] data (nine total sites, Table 1) and evaluated these data at the daily time step. Data were sourced from open access data portals: NV-H, NV-M, and NV-L from https://nevcan.dri.edu/data_download.html, NM-Hp and NM-Hb from <https://doi.org/10.17190/AMF/1246122>, NM-M from <https://doi.org/10.17190/AMF/1246121>, and AZ-H, AZ-M, and AZ-L from <https://data.sega.nau.edu/seg-aWeb/index.jsp>. We obtained PRISM Climate Group 4 km monthly P estimates from 2003 to 2019 for each site (15 yr; www.prism.oregonstate.edu; PRISM Climate Group at Oregon State University, 2004), which allowed us to determine wet and dry seasons and year by comparing site data to longer-term PRISM estimates.

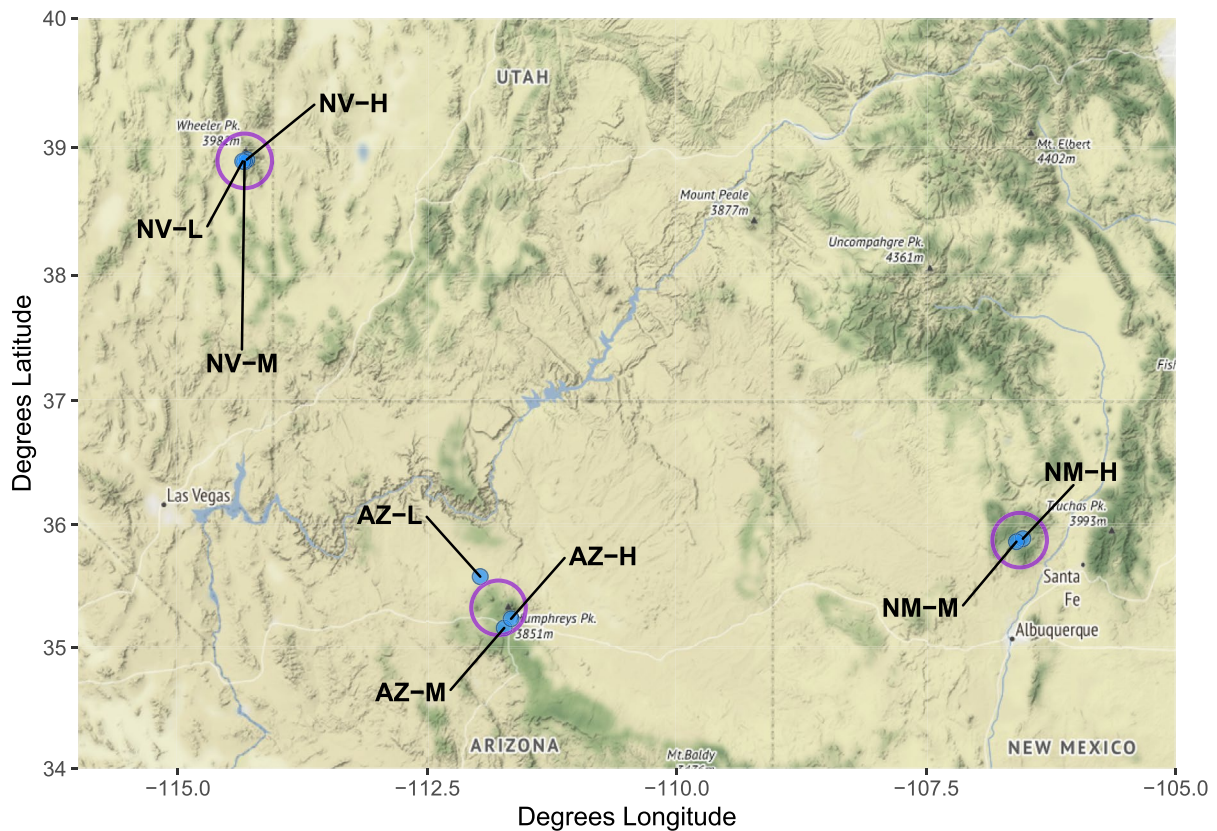


Figure 1. Site locations (blue) and areas of snow water equivalent (SWE) estimates (purple).

We were interested in linking year to year variation in high elevation snowpack to soil moisture at lower elevations, yet station-based snowpack monitoring data from United States Department of Agriculture Natural Resources Conservation Service Snow Telemetry (SNOTEL) sites did not comprise sufficient site-years for a robust comparison among study locations. We instead obtained Snow Data Assimilation System (SNODAS) 1 km² daily snow water equivalent [SWE: mm] estimates for a regional area of 25 km² surrounding the centroid of each elevation gradient from 2003 to 2019 (15 yr; <https://nsidc.org/data/g02158>; National Operational Hydrologic Remote Sensing Center, 2004). We averaged the top 25th percentile of cells to estimate SWE at the highest elevations at each of our study locations in each year. SWE estimates therefore reflect the expected snowpack at high elevation locations within each of our three elevation gradients, which is similar to data that obtained from SNOTEL monitoring stations, and not to snowpack at any individual site.

We categorized P totals in each season at each site using site rainfall data, long-term PRISM data, and snowfall estimates: above-average (>+25% long-term average), near-average (from +25% to -25%), and below-average (<-25%; Table 2). To categorize winter P at each site, we compared maximum observed SWE in each year to average maximum SWE from 2003 to 2019 using SNODAS estimates. To categorize spring and summer precipitation at each site, we compared site-measured total P in each season to the average total P from 2003 to 2019 from PRISM.

We obtained soil moisture [θ : mm³ mm⁻³] data and evaluated these data at the daily time step. Data were sourced from open access data portals: NV-H, NV-M, and NV-L from https://nevcan.dri.edu/data_download.html, NM-Hp and NM-Hb from <https://doi.org/10.17190/AMF/1246122>, NM-M from <https://doi.org/10.17190/AMF/1246121>, and AZ-H, AZ-M, and AZ-L from <https://data.sega.nau.edu/segaWeb/index.jsp>. We did not gapfill θ data, and excluded 2012 at NV-H and 2011 at NM-Hp from our analysis due to large θ gaps. Because θ measurement depths differed across sites, we standardized θ data to 0–10 cm and 10–20 cm depths using weighted averages determined through linear interpolation (Hengl et al., 2014). We

Table 2

Average P Experienced at Each Site Over 15 Years and During Data Collection (Study Period)

Site	15-yr Max SWE (mm)	15-yr spring P (mm)	15-yr summer P (mm)	Study Max SWE (mm)	Study Spring P (mm)	Study Summer P (mm)	Winter	Spring	Summer
NV-H	150	210	100	150 (0%)	150 (−29%)	90 (−10%)	W: 2/6 D: 3/6	W: 0/6 D: 4/6	W: 1/6 D: 3/6
NV-M	150	130	80	140 (−7%)	140 (+8%)	80 (0%)	W: 2/7 D: 3/7	W: 2/7 D: 3/7	W: 2/7 D: 2/7
NV-L	150	130	80	140 (−7%)	100 (−23%)	70 (−13%)	W: 2/7 D: 3/7	W: 0/7 D: 4/7	W: 2/7 D: 4/7
NM-Hp	200	140	220	250 (+25%)	160 (+14%)	210 (−5%)	W: 2/5 D: 0/5	W: 2/5 D: 0/5	W: 0/4 D: 0/4
NM-Hb	200	140	220	130 (−35%)	90 (−36%)	220 (0%)	W: 0/5 D: 3/5	W: 0/5 D: 3/5	W: 0/5 D: 0/5
NM-M	200	120	200	180 (−10%)	80 (−33%)	180 (−10%)	W: 2/11 D: 4/11	W: 1/11 D: 8/11	W: 0/11 D: 3/11
AZ-H	170	70	200	150 (−12%)	130 (+86%)	320 (+60%)	W: 1/3 D: 0/3	W: 2/3 D: 1/3	W: 3/3 D: 0/3
AZ-M	170	80	200	150 (−12%)	40 (−50%)	140 (−30%)	W: 1/3 D: 1/3	W: 0/3 D: 3/3	W: 0/3 D: 3/3
AZ-L	170	60	170	150 (−12%)	30 (−50%)	100 (−41%)	W: 1/3 D: 1/3	W: 0/3 D: 3/3	W: 0/3 D: 2/3

Note. Site averages were calculated from 15 years (2003–2018) of SNODAS data for maximum SWE (National Operational Hydrologic Remote Sensing Center, 2004) and PRISM data for spring and summer P (PRISM Climate Group at Oregon State University, 2004). The study period averages were calculated from measurements collected at each site and the difference between the study period average and the 15-year site average is noted. The presence of wet (W; $P > +25\%$ long-term average) and dry (D; $P < -25\%$ long-term average) seasons are noted by the fraction of abnormally wet or dry seasons in the study period.

also evaluated θ data at 50 cm for three sites in the NMEG gradient. Because θ is influenced by soil water holding capacity, we standardized θ across sites by calculating relative extractable soil moisture (θ_r) from soil properties as:

$$\theta_r = \frac{\theta - \theta_{min}}{\theta_s - \theta_{min}} \quad (1)$$

where θ_s is saturated soil water content calculated from Saxton and Rawls (2006). We obtained estimates of physical soil characteristics (% Sand, % Clay, and % Organic material) for each site from SoilGrids (soilgrids.org; Hengl et al., 2014). Physical soil equations related to water holding capacity, including those from Saxton and Rawls (2006), often overestimate the soil hygroscopic point, which is the theoretical minimum θ value used to calculate θ_r . Thus, in many cases observed θ is lower than the theoretical minimum. To correct this, we calculated θ_r from θ_s and the lowest observed θ value at each site (θ_{min}).

3.2. Time-Varying Characterization of Seasonal Soil Moisture

Seasons defined by month (e.g., summer from June–August in every year) have limited ability to detect variation in θ , that characterizes seasonal wetness or dryness. For example, in a year with a wet spring and a dry summer, seasons defined by month may not capture the transition between soil moisture availability and deficit, and would therefore underestimate moisture availability in spring and overestimate it in summer. To capture this variability and to assess θ -defined seasons, we developed time-varying conditions to capture

seasonal θ_r patterns at the daily time step independently for each site, in each year, and at each depth in the soil profile (Figure 2a). We sought to define three distinct seasonal periods: (1) a winter season when P was stored aboveground as snow, and moisture infiltration into the soil profile was very low; (2) a spring season that began at the onset of sustained snowmelt infiltration into the soil profile and ended when winter (snowfall) and spring (rainfall) θ inputs were depleted; and (3) a summer season when θ inputs were dependent on rainfall events. In our analysis, θ -defined winter is December until the beginning of snowmelt recharge (Si), spring is the snowmelt input period from Si to the day of snowmelt depletion (Sd), and summer is the period after Sd when θ_r is dependent on rainfall events (Figure 2a). We did not use this technique to identify a fall season, which we expect to resemble summer conditions but to be largely influenced by seasonal temperature change, reduction of vapor pressure deficit, and the initiation of snow accumulation. For this reason, we did not expect that θ patterns would be an appropriate way to characterize interannual patterns of fall at our study sites.

Snowmelt input (Si) is the day in spring when soil moisture begins to increase from melting snow, calculated by finding the first of five consecutive days of the water year in which θ_r is greater than the winter (DJF) average θ_r for that water year. Snowmelt peak (Sp) is the DOY and magnitude of maximum θ_r prior to DOY 180. Snowmelt depletion (Sd) is the DOY when θ_r becomes reliant on rainfall, calculated as the first day after Sp when θ_r is \leq the summer (JJA) mean θ_r . Snowmelt time (St) is the number of days between Si and Sd . Length of summer (L) is the number of days when θ_r is dependent on rainfall, calculated as the number of days between Sd and DOY 305 (Oct 1). DOY 305 was chosen as a day representative of the general cooling temperatures of late fall into winter and the end of the growing season in the SWUS. P input as moisture into the soil is the amount of volumetric water content increase, rather than standardized θ_r increase or P readings from a rain gauge, at each site during the summer L , reported as total summer P input. These measures could be identified in all sites and site-years, with the exception of Si at AZ-L and NV-L, which could not be identified because of ephemeral snowpack and continuous snowmelt.

Our analysis also focused on the properties of dry days (D_x) in summer. We calculated the number of days when θ_r was $<2\%$, $<5\%$, $<10\%$, $<20\%$, and $<$ the site summer mean ($\bar{\theta}_r$) during the summer period L . Days with $\theta_r < 20\%$ ($D_{<20}$) was the most transferable of dry day metrics because this value fell consistently below summer mean θ_r at all sites. Our analysis therefore focuses on $D_{<20}$ but includes other measures of dry days in Tables A1, A2, and A3.

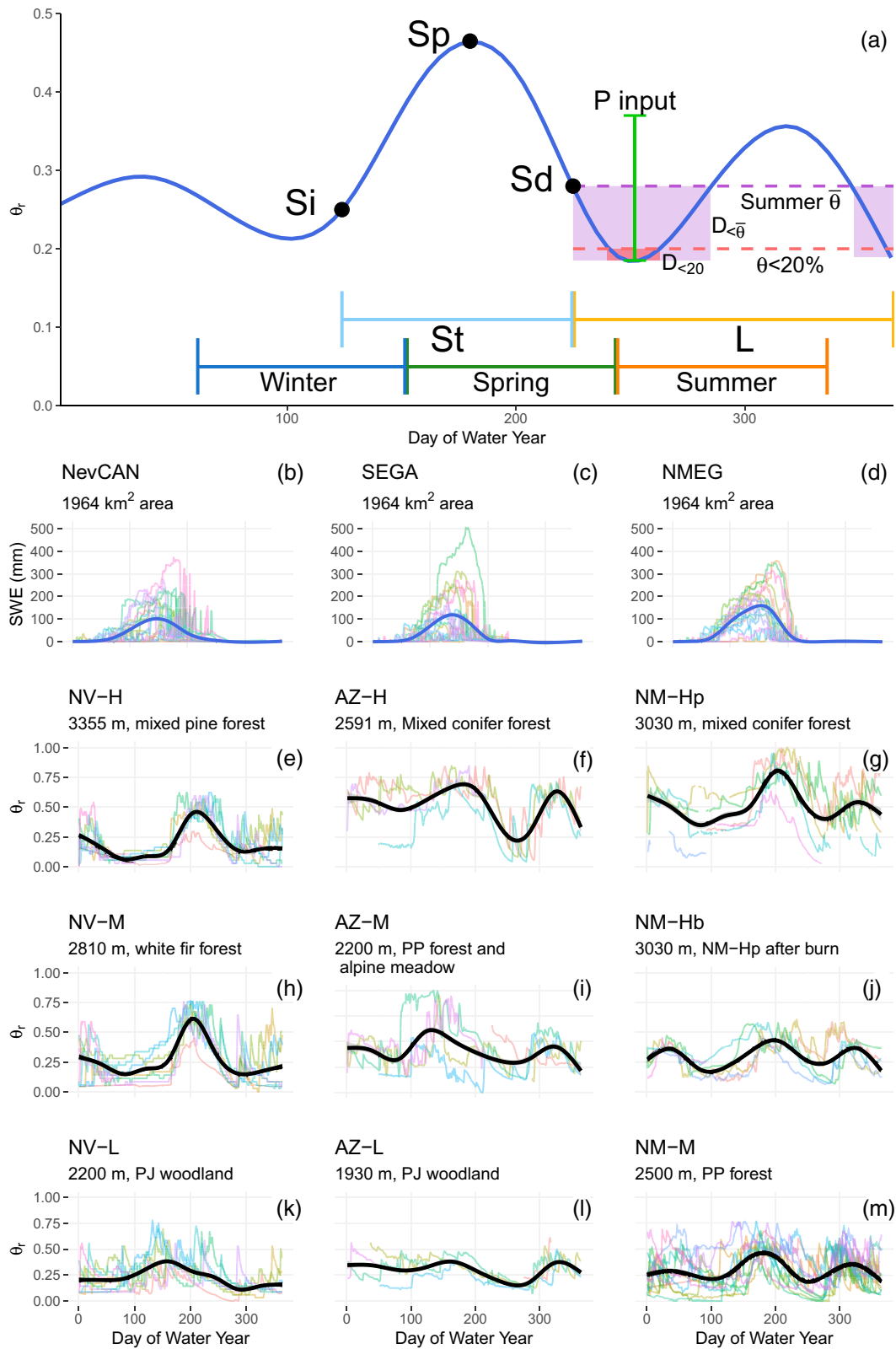
3.3. Correlations in Soil Moisture Patterns

We used univariate linear models to test the influence of meteorological events, environmental factors, and seasonal characteristics of θ_r at each soil depth, pooled across all sites and years. We compared all seasonal variables (maximum SWE DOY, Si DOY, Sp DOY, Sd DOY, St , and L) and moisture volume variables (maximum SWE, Si θ_r , Sp θ_r , Σ P input, $D_{>\bar{\theta}}$, $D_{<\bar{\theta}}$, $D_{<20}$, and $D_{<10}$) to each other using correlation coefficients at the $p < 0.05$ level (Tables A1, A2, and A3).

3.4. Soil Moisture Relationships Across Depths in the Soil Profile Using Transfer Entropy

We used information theory to quantify similarity between the probability distributions of θ_r between shallow (0–10, 10–20) and deeper (10–20, 50 cm) depths in the soil profile. Transfer entropy (TE) quantifies the amount of information in a time series of variable X that can be used to predict the response of variable Y in a co-occurring time series at either the same point in time ($t = 0$) or at a future point in time ($t = n$). TE specifically quantifies the amount of uncertainty reduced in estimating variable Y at time t given complete knowledge of variable X, and has been used successfully to examine nonlinear θ dynamics through time (Behrendt et al., 2019). We calculated TE using the package RTransferEntropy in R software (Behrendt et al., 2019; R Core Team, 2019).

We calculated TE ($t = 0$) for θ_r between shallow and deeper soil depths at each site and in each season independently. To calculate TE, data must be discretized into bins. Our default number of bins was 25 of equal width in the range of the data, and we reduced this number when it was required for accurate calculation of TE. To reduce biased estimates, we removed any TE calculations with <5 bins from our analysis. We determined statistical significance at the $p < 0.05$ level using a Markov block bootstrapping technique



with 300 replications, and only report significant relationships between variable X and variable Y (Behrendt et al., 2019). Our analysis reports significant TE values between θ_r at shallower (variable X) and deeper (variable Y) soil profile depths, categorized as occurring within wet, dry, and average winter, spring, and summer seasons. Thus, our TE analysis quantifies to what degree shallow θ_r informs θ_r at deeper soil depths in wet, dry, and average seasons across all of the sites in our study.

3.5. Soil Moisture Relationships Across Seasons Using Information Theory

We also used information theory to quantify similarity between the probability distributions of θ_r and SWE between seasons. To do this, we calculated two variables, mutual information (MI) and Kullback-Leibler divergence (K-L), to compare the probability distributions of variable X and variable Y in different seasons. MI is a measure of the decrease in uncertainty generating an unknown probability distribution (variable Y) from another known distribution (variable X), and in our analysis was quantified as the number of bits needed to generate a point in the unknown Y time series given complete knowledge of the distribution of X (Hausser & Strimmer, 2009). K-L is a measure of “surprise” in generating an unknown probability distribution (variable Y) from another known distribution (variable X), with the prior assumption that X and Y are identical (Hausser & Strimmer, 2009; Pérez-Cruz, 2008). Higher K-L values indicate a greater “surprise” at the difference between the X and Y density distributions, and in our analysis were quantified as the number of extra bits needed to generate a point in the Y distribution because it is not actually identical to the X distribution. High similarity (e.g., both low MI and low K-L values for the distributions of variable X and variable Y) potentially indicates a common mechanism or shared physical driver.

We calculated K-L and MI between seasonal (time-varying winter, spring, summer) SWE and θ_r distributions. This analysis computed the shared information of distributions of SWE and soil moisture between two seasons in the same year, which when calculated across a large number of years provides insight on which seasons and associated P conditions (wet, dry, and average) are more closely linked than others. We conducted our analysis independently for each year, site, and soil depth. θ_r data were discretized into the maximum number of bins (>5 and < 25) in which at least one probability distribution had no bins containing 0 observations. Seasons were classified as dry, average, or wet based on total P and maximum SWE. In our analyses, we defined relationships between two density distributions, such as θ_r at 0–10 cm in spring (season X) compared to θ_r at 0–10 cm in summer (season X + 1), that had both below-average MI and below average K-L (compared to all other θ_r relationships) as having high similarity. We calculated MI and K-L using R package entropy (Hausser & Strimmer, 2009).

4. Results

4.1. Time-Varying Analysis of Forest and Woodland Seasonality

Our time-varying analysis identified three distinct seasonal periods: (1) a winter season when P was stored aboveground as snow, and moisture infiltration into the soil profile was very low; (2) a spring season that began at the onset of sustained snowmelt infiltration into the soil profile and ended when winter (snowfall) and spring (rainfall) θ inputs were depleted; and (3) a summer season when θ inputs were dependent on rainfall events (Figure 2, see Figure B1 for these patterns at 10–20 cm and 50 cm). Compared to month-based seasons, time-varying seasons generally result in a longer winter and summer and a shorter spring, with variation in the length of these seasons from year to year and across different depths in the soil profile

Figure 2. Summary of time-varying analysis of relative extractable soil moisture [θ_r ; $\text{mm}^3 \text{mm}^{-3}$] for (a) one hydrologic year, (b–d) time series plots of estimated snow water equivalent SWE [mm] for each elevation gradient, and (e–m) observed θ_r at 0–10 cm for all sites starting on October 1, the start of the hydrologic (water) year (Biederman et al., 2018; Ma et al., 2007; Thomas et al., 2009). In (a), S_i (snowmelt input) is the DOY when θ_r begins to increase from melting snow, S_p (snowmelt peak) is the DOY and magnitude of maximum θ_r in the spring, S_d (snowmelt depletion) is the DOY when θ_r becomes reliant on rainfall for replenishment, S_t (snowmelt time) is the number of days when melting snow is infiltrating into the soil profile, L (length of summer) is the number of days where θ_r is dependent on rainfall events, D_x (dry days) is the number of days where $\theta_r <$ the summer mean ($\bar{\theta}$) or $\theta_r <$ 20% of soil capacity, and P input tracks rainfall infiltration into the soil profile. Month-defined winter, spring, and summer are shown for reference. In (e–m), colored lines illustrate θ_r in individual years, and the black lines illustrate a smoothed trend.

Table 3
Moisture Transition Patterns by Site Including Snowmelt Input Day (*Si* Water Year DOY), Snowmelt Peak Day and Amount of Moisture (*Sp* Water Year DOY and θ_r), Depletion Day (*Sd* Water Year DOY), Snowmelt Time (*St*), Days With $\theta_r < 20\%$ ($D_{<20}$), and Summer Moisture Input (ΣP Input, mm)

Site	<i>Si</i> WY DOY	<i>Sp</i> θ_r 0–10 cm	<i>Sp</i> θ_r 10–20 cm	<i>Sp</i> θ_r 50 cm	<i>Sd</i> WY DOY 0–10 cm	<i>Sd</i> WY DOY 10–20 cm	<i>Sd</i> WY DOY 50 cm	<i>St</i> (days)	$D_{<20}$ 0–10 cm	$D_{<20}$ 10–20 cm	$D_{<20}$ 50 cm	ΣP input
NV-H	158 ± 9	0.54 ± 0.06	0.56 ± 0.03	ND	248 ± 24	269 ± 8	ND	90 ± 27	49 ± 36	91 ± 24	ND	35 ± 8
NV-M	163 ± 3	0.69 ± 0.11	0.69 ± 0.16	ND	262 ± 11	263 ± 24	ND	99 ± 11	91 ± 30	73 ± 51	ND	42 ± 15
NV-L	N/A	0.63 ± 0.14	0.53 ± 0.13	ND	242 ± 66	217 ± 59	ND	176 ± 74	134 ± 33	159 ± 32	ND	31 ± 24
NM-Hp	165 ± 11	0.89 ± 0.15	0.91 ± 0.11	0.82 ± 0.03	254 ± 27	257 ± 26	258 ± 15	89 ± 35	0	0	0	60 ± 23
NM-Hb	156 ± 9	0.54 ± 0.07	0.51 ± 0.08	0.46 ± 0.07	245 ± 26	244 ± 21	261 ± 49	88 ± 30	44 ± 37	60 ± 42	49 ± 46	33 ± 7
NM-M	157 ± 7	0.62 ± 0.13	0.62 ± 0.14	0.67 ± 0.23	221 ± 30	224 ± 33	241 ± 29	62 ± 35	72 ± 40	73 ± 46	60 ± 37	70 ± 20
AZ-H	156 ± 7	0.80 ± 0.07	0.81 ± 0.08	ND	236 ± 9	240 ± 10	ND	80 ± 15	31 ± 8	38 ± 6	ND	83 ± 24
AZ-M	113 ± 40	0.83 ± 0.26	0.77 ± 0.35	ND	168 ± 44	202 ± 53	ND	75 ± 80	48 ± 46	31 ± 31	ND	101 ± 37
AZ-L	N/A	0.45 ± 0.04	0.38 ± 0.11	ND	188 ± 45	198 ± 57	ND	128 ± 45	69 ± 30	72 ± 45	ND	46 ± 1

Note. Water year begins October 1. All metrics given in this table are given with the mean \pm SD and are for soil depth 0–10 cm unless stated otherwise. ND, no data.

(Table 3, Figure 3, Figure 2e–2m for moisture traces at 0–10 cm, Figure B1 for moisture traces at 10–20 and 50 cm). This seasonal framework applied to all site-years. NV-L and AZ-L, which were low elevation woodlands that experienced ephemeral snow accumulation and sporadic snowmelt during our study, had a longer spring season than other sites and no winter season defined by a single day of snowmelt initiation (Table 3).

4.2. Seasonal Relationships of High and Low Elevation Sites

We found significant differences in the characteristics of winter, spring, and summer between low elevation sites (<2,500 m: AZ-L, AZ-M, NV-L, and NM-M) and high elevation sites (>2,800 m: NV-M, NM-Hp, NM-Hb, and NV-H; $p < 0.05$). The DOY of snowmelt initiation (*Si*, see Figure 2a for a reference), which indicates the transition from winter to spring, was 9 days earlier on average at low elevation sites compared to high elevation sites (Table 3). The DOY of peak θ_r due to snowmelt (*Sp*) at low elevation sites occurred 45 days earlier than at high elevation sites (Figure 4a, Table 3). The DOY of θ_r depletion (*Sd*), which indicates the transition from spring to summer, occurred 34 days earlier at low elevation sites than at high elevation sites, and corresponded to a 34 day longer summer (*L*; Figure 4c and 4e, Table 3). θ_r at the snowmelt peak, the length of spring, and the number of days with <20% θ_r ($D_{<20}$) did not vary significantly between high and low elevation sites, and was instead influenced by year to year variation in rainfall at individual sites (Figure 4b, and 4d, 4f).

Seasons with above- and below-average P (e.g., wet and dry seasons) had consistent effects on some of the characteristics of winter, spring, and summer for both low and high elevation sites. The DOY of peak θ_r due to snowmelt (*Sp*) occurred later in wet springs compared to dry springs at all sites, and both dry winters and dry springs resulted in lower peak θ_r in spring compared to corresponding wet conditions (Figure 5b–5d). Dry winters also corresponded to an earlier DOY of θ_r depletion (*Sd*) and a longer summer length (*L*) across all sites (Figure 5e and 5g). In contrast, spring length (*St*) and the number of days with <20% θ_r ($D_{<20}$) were not consistently altered by P totals (Figure 5a, 5f, and 5h).

4.3. Soil Moisture Information Across Depths in the Soil Profile

TE quantifies how temporal change in variable X informs temporal change in a second variable, Y (higher positive TE values indicate more information transfer from X to Y). We used TE to determine how θ_r in upper soil layers informed θ_r at a deeper soil layer at the same site during the same seasons (see Figure B2 for an expanded view of these findings for wet and dry seasons). TE was highest for θ_r between shallow soil layers (0–10 to 10–20 cm; Figure 6a). TE was lower for θ_r between a shallow soil layer X (0–10 or 10–20 cm) and a deeper soil layer Y (50 cm; Figure 6a). Compared to month-based seasons, TE in time-varying seasons was lower in winter and higher in spring and summer for transfer between shallow depths (0–10 to 10–20 cm; Figure 6b), which we attribute to better identification of seasonality in θ_r availability using a time-varying approach (relatively wetter and shorter springs, relatively drier, and longer summers).

Linear correlations of seasonal relationships attest to the differing seasonal patterns of θ_r between shallow and deeper soils, and corroborate our TE-based finding of relatively low similarity in θ_r patterns between these soil depths. For θ_r at 0–10 and 10–20 cm, SWE was correlated with spring measures including *Sp* θ_r and *Sd* DOY (Tables A1 and A2), whereas at 50 cm, SWE was correlated with *Sp* θ_r and summer wet and dry days (Table A3). Thus, although all soil depths are influenced by SWE in

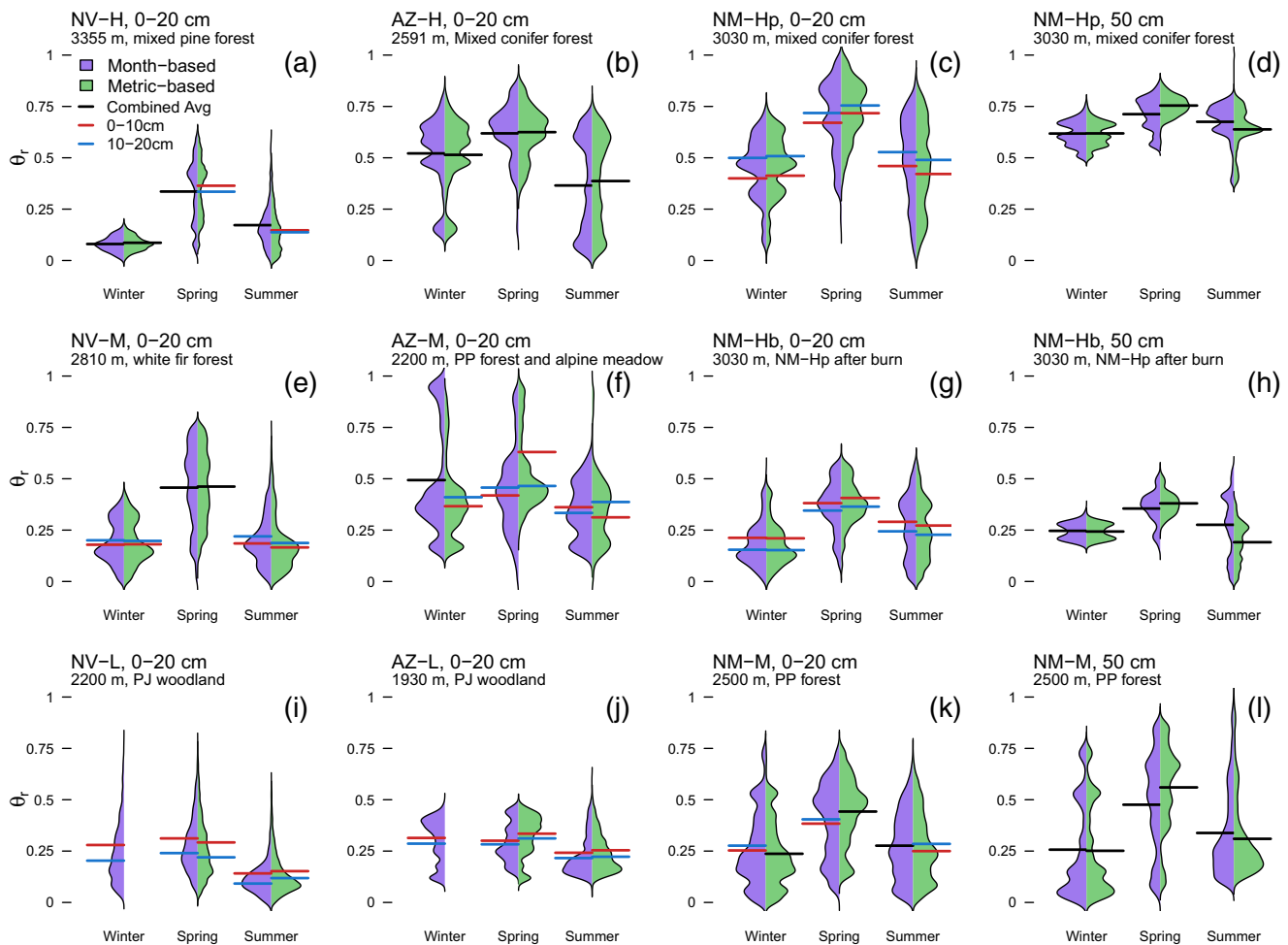


Figure 3. Probability density distributions of θ_r at 0–20 and 50 cm depths contrast seasons defined by months (Winter: DJF; Spring: MAM; and Summer: JJA) to those defined by θ -based metrics. Horizontal lines indicate the average of the probability density functions. The combined average of depth 0–10 cm and depth 10–20 cm was used if the averages were not significantly different ($p < 0.05$). (i) NV-L and (j) AZ-L did not experience constant snowpack and a single day of snowmelt initiation and thus do not have θ -based winter seasons.

spring, the effect of variable winter precipitation on θ_r , persists for longer in deeper layers (summer) versus shallow soil layers (spring), leading to their observed dissimilarity.

4.4. Seasonal Relationships of Soil Moisture Information Between Seasons and Across Depths in the Soil Profile

We used information theory to determine how θ_r in season X informed θ_r in season X + n at the same depths in the soil profile. MI between two variables (X and Y) quantifies the amount of additional information needed to encode the distribution of Y values given complete information on the distribution of X values. Kullback-Leibler divergence (K-L) quantifies the deviation between the shared distributions of X and Y, given the assumption that their distributions are identical. Our analysis focused on seasonal θ_r classes (spring θ_r at 0–10 cm to summer θ_r at 0–10 cm, for example) with lower than average MI (less additional information needed) and K-L (lower divergence), and therefore high shared information. The percentage difference in our MI and K-L analysis indicates a greater or lesser proportion of high shared information for a specific class of observation compared to that class's proportion of all observations (for example, the proportion of high shared information at 0–10 cm depth to high shared information across all depths (27/54, 50%), compared to the proportion of 0–10 cm observations compared to all observations (224/542, 41%). Therefore, a positive difference between the percentage of one observation class in all observations (e.g., 41%) and in

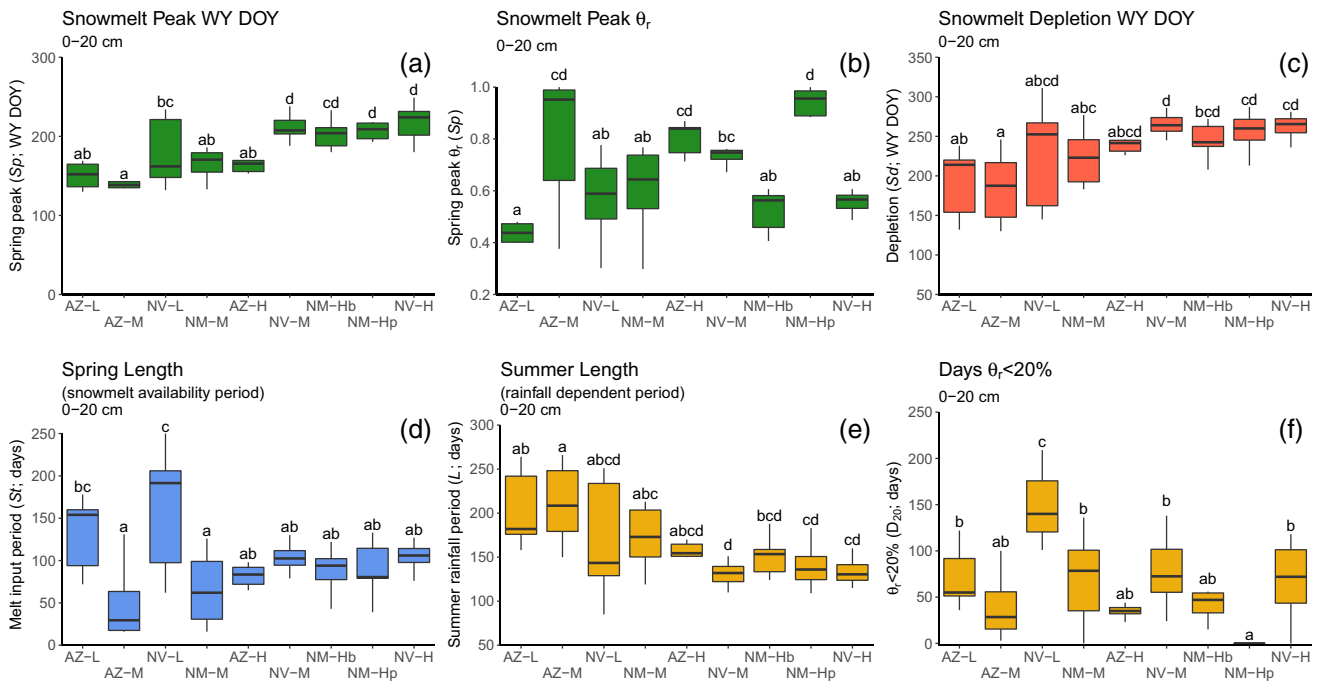


Figure 4. Time-varying soil moisture measures of snowmelt peak day (Sp Water Year DOY, 0–20 cm; a), snowmelt peak relative extractable soil moisture [θ_r ; $\text{mm}^3 \text{mm}^{-3}$] ($Sp \theta_r$, 0–20 cm; b), depletion day (Sd Water Year DOY, 0–20 cm; c), snowmelt time (St , 0–20 cm; d), summer length (L , 0–20 cm; e), and days with $\theta_r < 20\%$ ($D_{<20}$, 0–20 cm; f). Water year begins on October 1. Letters indicate significant differences between sites ($p < 0.05$). AZ-L and NV-L did not experience snowpack, so their St is defined as the beginning of winter until Sd . Metrics were not significantly different at depths 0–10 and 10–20 cm, so the two depths were merged to 0–20 cm. All significance levels were found using ANOVA and Tukey’s honest significant differences.

observations with high shared information (e.g., 50%) indicates a higher likelihood of high shared information within that class (θ_r comparisons at 0–10 cm). Generally, cases of high shared information were rare (9% of all season X to season X + n comparisons). Distributions of θ_r between seasons have slightly higher shared information at 0–10 cm, and slightly lower shared information at 50 cm (Figure 7a). Across all soil depths, the highest proportional increase in high information seasonal relationships were between θ_r in spring and summer (+23%), θ_r in winter and summer (+12%), and θ_r in winter and spring (+7%; Figure 7b, see Figure B3 for an expanded view of these findings). Relationships between SWE and θ_r were much lower (Figure 7b). Events of high shared information were most likely to occur when season X (winter or spring) was dry (+8%) or wet (+6%), and when season X + n (spring or summer) experienced average rainfall totals (+18%; Figure 7c).

Linear correlations of seasonal relationships corroborate our finding of high shared information between spring and summer for shallow soil layers. At 0–10 and 10–20 cm, $Sp \theta_r$ is significantly correlated with Sd day, summer length L , and several measures of wet and dry days (Tables A1 and A2). At 50 cm, $Sp \theta_r$ is correlated with summer wet days, which supports our finding of high shared θ information between spring–summer at this deeper soil depth (Table A3). Additionally, although we found that SWE was significantly correlated with $Sp \theta_r$ at every soil depth, SWE was not correlated with additional seasonal measures, supporting our finding that SWE impacts in late spring and summer may be limited to deeper depths in the soil profile (Table A3).

5. Discussion

5.1. Time-Varying Metric-Derived Seasons

Distinct seasonal cycles of θ have been evaluated in numerous studies for ecosystems of the western United States (Brown-Mitic et al., 2007; McNamara et al., 2005; Notaro et al., 2010; Williams et al., 2009). By determining the seasonal characteristics of θ using a time-varying, quantitative methodology, our study provides new insight on climate and soil moisture dynamics for sites spanning three forest to woodland elevation

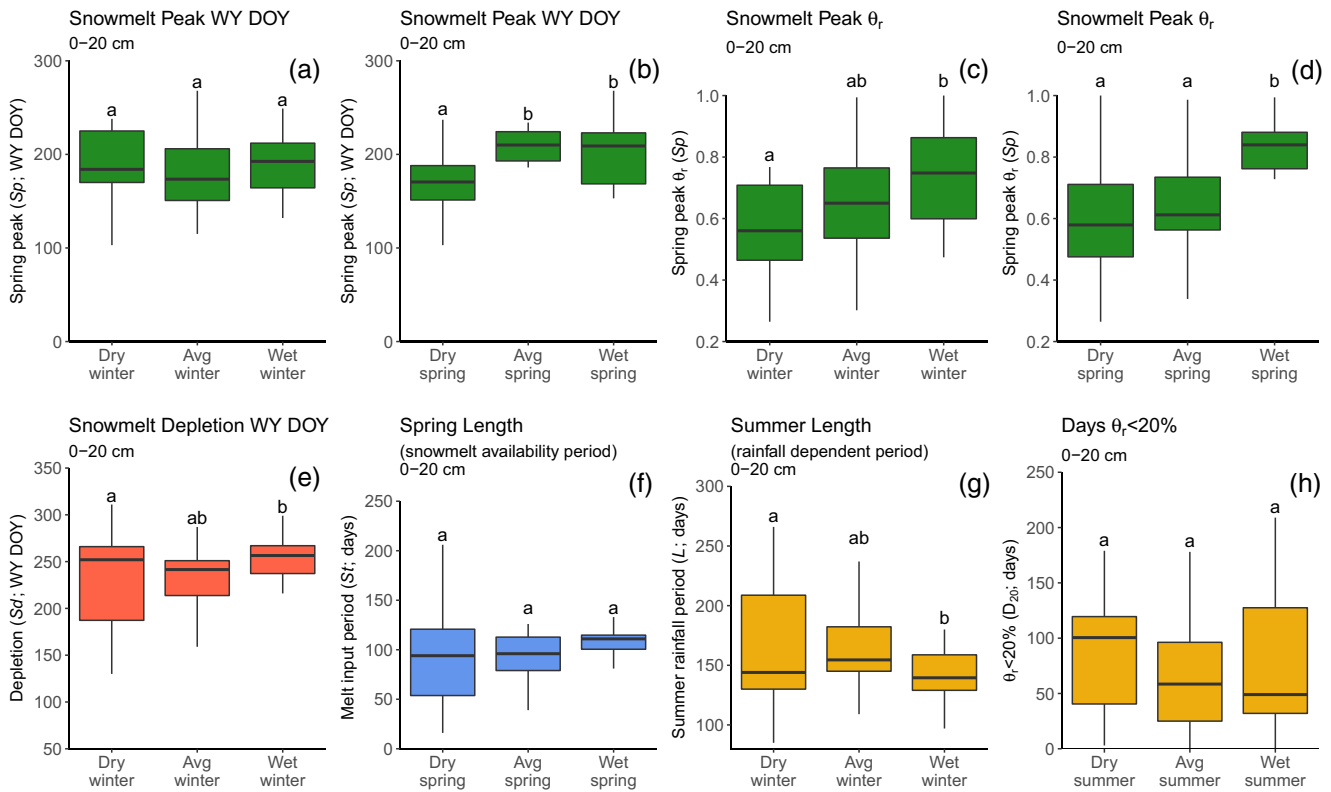


Figure 5. Time-varying soil moisture measures of snowmelt peak day (Sp Water Year DOY, 0–20 cm; a, b), snowmelt peak relative extractable soil moisture ($Sp \theta_r$, 0–20 cm; c, d), depletion day (Sd Water Year DOY, 0–20 cm; e), snowmelt time (St , 0–20 cm; f), summer length (L , 0–20 cm; g), and days with $\theta_r < 20\%$ ($D_{<20}$, 0–20 cm; h) across above-average (wet), below-average (dry), and near average (avg) seasonal P totals (winter, spring, or summer). Water year begins on October 1. We compared all site-years to identify patterns of responses to P that are similar across the region and responses without a clear pattern that reflect responses shaped by environmental differences among sites. Letters indicate significant differences between sites ($p < 0.05$). Metrics were not significantly different at depths 0–10 and 10–20 cm, so the two depths were merged to 0–20 cm. All significance levels were found using ANOVA and Tukey’s honest significant differences ($p < 0.05$).

gradients in the SWUS with distinct climate characteristics. Specifically, our study provides new insight on how θ patterns in these ecosystems compare across depths in the soil profile, between winter, spring and summer seasons, and under climate forcing conditions of above- and below-average seasonal P. We used time-varying methodology to define a distinct winter period of snow accumulation and low snowmelt, a spring period of high, mostly snow-derived moisture availability, and a summer period of relative moisture deficit. Compared to month-defined seasons, time-varying seasons were able to more precisely identify the

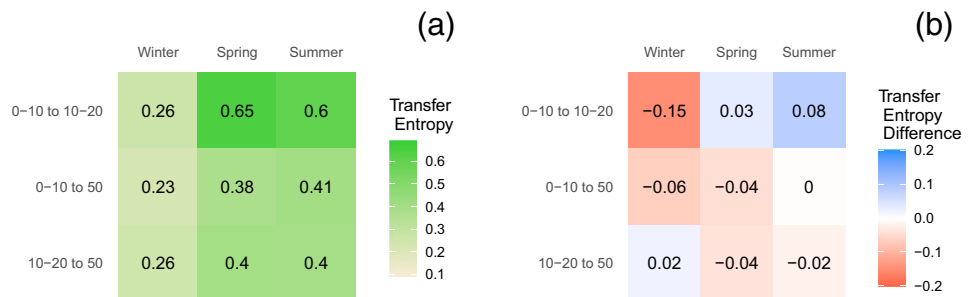


Figure 6. Transfer entropy (TE) values of relative extractable soil moisture [θ_r ; $\text{mm}^3 \text{mm}^{-3}$] for (a) time-varying seasons between 0–10, 10–20, and 50 cm soil depths, and (b) TE compared between time-varying, metric-based seasons and month-based seasons (metric-based TE minus month based TE). In (a), higher TE values indicate greater information transfer between soil layers.

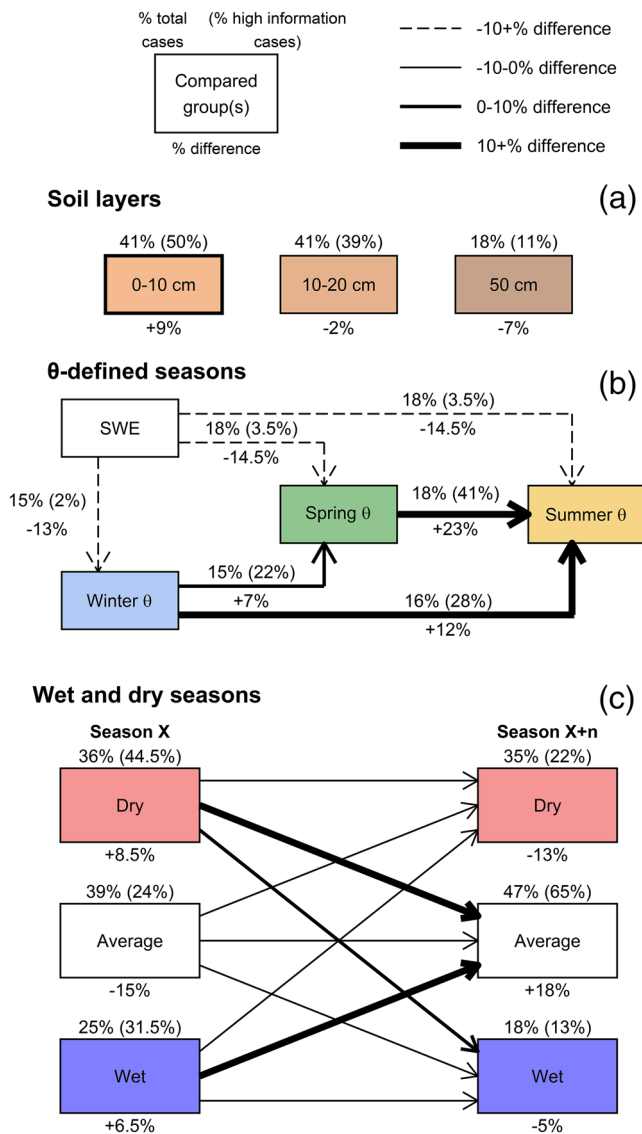


Figure 7. Percentage of conditions with high mutual information content and Kullback-Leibler divergence (assessed using mutual information content and Kullback-Leibler divergence) for (a) relative extractable soil moisture [θ ; $\text{mm}^3 \text{mm}^{-3}$] at different depths in the soil profile, for (b) snow water equivalent [SWE; mm] and θ , across winter, spring, and summer, and between primary seasons (winter, spring) and subsequent seasons (spring, summer) with below-average (Dry), near average (Average), and above-average precipitation (Wet); c). In each panel, the value outside parentheses indicates the percentage of total observations for each condition, and the value inside parentheses indicates the percentage of total observations with high mutual information for each condition. The lower value indicates the difference between the two, illustrating a greater or lower tendency of observed conditions to have high mutual information; the thickness of box perimeters (a) and arrows (b and c) also indicates this value.

seasonal transition from moisture surplus in spring to moisture deficit in summer, and therefore are a useful approach to determine the functional length of these seasons as well as the magnitude of θ , availability within them. Due to the simplicity of this approach, we propose that time-varying θ analysis based on θ fluctuations may have broad utility for understanding the seasonal characteristics of these and other semiarid ecosystems, as well as for predicting how climate change may alter seasonal cycles of moisture availability.

Our proposed framework has a divergent but useful application in sites with ephemeral snowpack, such as NV-L and AZ-L, compared to sites that experience snow accumulation throughout winter. In our analysis, low elevation pinyon-juniper sites did not experience a single day that marks the beginning of snowmelt infiltration, but rather experience snowmelt infiltration throughout the cold season. Therefore, according to our proposed framework, these sites do not have a winter season of snow accumulation and instead experience an extended spring. We postulate that temperature variation during an extended θ -defined spring is higher than temperature variation in discrete winter and spring seasons, and may play an important role in regulating ecosystem responses that we did not resolve in this study. Despite this, we maintain that highlighting the potential increased role of temperature at lower elevation sites supports the value of our proposed framework, in addition to its ability to identify divergent seasonal P- θ relationships across diverse forest and woodland sites.

5.2. Effects of Elevation on Soil Moisture

Instead of differing across dominant vegetation species or ecosystem type, the seasonal characteristics of our study sites were often best categorized into two groups by elevation: <2,500 m (lower elevation) and >2,800 m (higher elevation). DOY of peak θ , due to snowmelt and the DOY of θ , depletion in spring were especially useful for differentiating the seasonal characteristics of high versus low elevation sites. Notably, lower elevation sites experienced a loss of snowmelt-derived θ , earlier in the year compared to higher elevation sites, and had a longer summer period where θ , was dependent on rainfall events. Additionally, variance in the timing of snowmelt inputs and depletion is much lower at high elevation mixed conifer and ponderosa forests compared to low elevation ponderosa forests and pinyon-juniper woodlands. This suggests a divergence in predominant climate and θ -defined seasons between lower and higher elevation sites in the SWUS, albeit with some uncertainty about the role of topographic and landscape effects that can amplify and dampen the effects of climate forcings. Our determination agrees with Herrmann et al. (2016), who found a distinct difference in seasonal NDVI patterns between lower and higher elevations in the SWUS, which were attributed to water- versus energy-limited conditions. Yet, we found that seasons with above-average and below-average P had consistent effects on many of the seasonal characteristics of both our lower and higher elevation sites, and that the number of dry days in summer was strongly controlled by site-specific factors. Thus, we postulate that differences in

solar radiation and temperature imparted some influence on the availability of snowmelt-derived soil moisture between the lower and higher elevation sites of our study, although precipitation remained the dominant control on seasonal soil moisture dynamics.

Climate change is predicted to increase temperatures and initiate earlier snowmelt in forest and woodland ecosystems of the western United States (Blankinship et al., 2014; Hamlet et al., 2007). Whether or not lower elevation sites can be used to forecast the warmer and more arid future of higher elevation sites is not fully clear and depends on many interesting factors (Bell et al., 2014). If lower elevation sites do indeed resemble the future of higher elevation sites, comparing existing patterns of θ availability between these elevations may be especially useful for refining understanding of the potential ecological consequences of climate change. For example, although the lower elevation sites of our study had shorter springs, longer summers, and were often drier than higher elevation sites, seasonal patterns of θ_r (increase in early spring, depletion in late spring, P-dependent summer) did not diverge markedly between them. Thus, seasonal patterns of θ availability are similar across less arid higher elevation and more arid lower elevation SWUS sites, although the magnitude of θ and the relative influence of seasonal P may differ. From a climate change perspective, this pattern suggests that the dynamic of lower elevation forest sites may indeed portend to the future of higher elevation forest sites, with the exception of nonanalog climate changes or infrequent climate events that are unobserved. However, we maintain that the role of topographic and landscape effects on site water balance, and potential change in the magnitude of environmental conditions that are ecologically meaningful, will also be important at both local and regional scales (Crausbay et al., 2017). We found that seasonal θ_r was much lower at the lowest elevation, pinyon-juniper woodland sites of our study. As we noted previously, these woodlands experience a major change in cold season moisture availability compared to higher elevation forests, as they do not often accumulate deep snowpack, and instead experience sporadic snowmelt and a very low θ_r peak throughout a long θ -defined spring. The transition from winter snowpack accumulation to snowpack melting is expected to have large impacts to ecosystems of the western US in the coming century, as this shift amplifies periods of spring and summer moisture deficit (Knowles et al., 2018; Petrie et al., 2015; Schlaepfer et al., 2012). Climate models predict that snowmelt in the SWUS will occur earlier and with less volume in this century (Seager & Vecchi, 2010), and lower elevation sites may be a useful model for the future of higher elevation sites, but only until winter snow accumulation becomes limited.

Our results suggest similarity in θ_r dynamics across three elevation gradients in the SWUS that span an elevational range of 1,930–3,355 m. Our results corroborate Herrmann et al. (2016) in that both identified a distinct divide between lower and higher elevation groups. Yet, studies focusing on elevation gradients at a finer-scale than those of our study have found gradual changes in streamflow (Hunsaker et al., 2012), conifer regeneration (Dodson & Root, 2013), and spring flowering timing (Crimmins et al., 2010). These results suggest fine-scale elevation-associated differences that we did not detect in our study. Because regionally focused studies such as ours are less able to identify fine-scale patterns, there could be an important moisture gradient within our low elevation sites. We conclude that further study of local and regional elevation gradients, as well as topographic and landscape effects on the ecological impact of climate patterns, is needed to continue to develop actionable generalization that applies across broad regional areas and can be used to predict future regional change in forest and woodland dynamics.

5.3. Shallow Versus Deeper Soil Moisture

Although P influenced θ at all of the sites and soil depths of our study, we found that θ_r at 0–20 cm is generally decoupled from θ_r at 50 cm and that there is limited statistical overlap between shallow and intermediate soil layers. This decoupling has been observed in other semiarid locations with a prominent snowfall season that can recharge θ throughout the soil profile, leading to a decoupling later in the year when shallow θ is depleted by evapotranspiration (Blankinship et al., 2014; Loik et al., 2004; McNamara et al., 2005). Although seasonal patterns of θ_r were similar between 0–10 and 10–20 cm at our study sites (though their means could differ), other semiarid forests in the SWUS experience differential soil moisture patterns between 0–10 and 10–20 cm due to evapotranspiration that is limited to the top 10 cm of the soil profile (Brown-Mitic et al., 2007; Newman et al., 1997). We caution that our results comparing shallow and intermediate soil moisture were obtained solely from the NMEG gradient. Other studies in our NV study region have found negligible deep soil moisture drainage in lower elevation woodlands, such that the primary seasonal contributions of drainage to groundwater occur only at mid-to high elevations (Devitt et al., 2018). Although this corroborates our findings at NMEG,

further study of local and regional elevation gradients is needed to continue to develop actionable generalization that applies across broad regional areas and can be used to predict future regional change in forest and woodland dynamics.

Despite noted limitations, we postulate that coupling of shallow and intermediate θ portends to a divergence in how different life stages of tree development are influenced by climate variability. Juvenile ponderosa pine do not have the ability to access soil moisture below 10–20 cm in the first years following germination (unpublished data), and soil moisture availability at this shallow layer has a large influence on juvenile survival (Petrie et al., 2017). Thus, the most likely impact of spring and summer climatic conditions that deplete soil moisture in upper soil layers is the reduction of natural regeneration in forest and woodland ecosystems. In contrast, adult ponderosa pines uptake water from the upper 50 cm of soil (Berndt & Gibbons, 1958), but rely more heavily on deeper soil moisture compared to young trees (Kerhoulas et al., 2013). In pinyon-juniper woodlands, the rooting profile of both pinyon pines and junipers is more concentrated in upper soil horizons (Schwinning et al., 2020). It follows that sustained periods of low θ recharge into intermediate and deeper soil layers may be especially deleterious for mature ponderosa pine systems (Zhang et al., 2013), whereas similar levels of stress to mature trees in pinyon-juniper ecosystems is manifest by sustained θ depletion in upper soil layers (Breshears et al., 2009). Additionally, changes to θ are also an important component of ecosystem recovery from disturbance, as moisture availability greatly affects the ability of seedlings to regenerate the forested ecosystem (Dodson & Root, 2013). Although our analysis sites capture conditions before and after a severe wildfire (NM-Hp and NM-Hb), P totals at this site were generally wetter than average before the fire and were drier after. This limited our ability to elucidate wildfire effects on θ dynamics.

5.4. Seasonal Information Flow in Wet and Dry Seasons

High information transfer between seasons may be associated with change to the physical relationships between climate and soil moisture. Greater information transfer between soil layers was promoted in wet seasons compared to average and dry seasons, especially wet winters. This may be due to both reduced soil drying in shallow soil layers and greater water inputs in total. Additionally, we found that in high elevation locations, where the day of snowmelt moisture input (S_i) could be identified, it was often placed after some infiltration had already taken place in wet years, whereas in dry years S_i was more accurate to the day when snowmelt input first appeared in the soil moisture trace. Thus, wet conditions may enhance information transfer between soil layers in our framework by simply allowing moisture infiltration into the soil, which is less likely under average or dry conditions. Our results corroborate Hupet and Vanclooster (2002) and Famiglietti et al. (1999), who found that variation in θ horizontally was lowest in wet conditions, but is in contrast with Williams et al. (2009) who found the opposite trend. These studies examine information flow horizontally across space rather than vertically through the soil profile, and while P influences both horizontal and vertical θ patterns, it is likely that additional mechanisms influence each flow type.

Climate change is predicted to alter seasonal P and θ dynamics in the SWUS, and these changes could intensify or dampen θ MI content (assessed by Kullback-Leibler divergence and MI) between seasons. Warmer, drier winters (Jones & Gutzler, 2016; Seager & Vecchi, 2010), and modestly drier summers (Jones & Gutzler, 2016) are expected to increase, and interannual precipitation is expected to become more variable, with extreme droughts (Cayan et al., 2010) and extreme wet periods (Allan & Soden, 2008) both becoming more likely. At the sites of our study, seasons with near-average P are more likely to be influenced by prior-season conditions. Both warming temperatures and a more variable P regime will change the likelihood of high MI content between seasonal θ signatures. The probability of a dry season X (winter, spring) or a dry season X + n (spring, summer) will increase, and forecasts for increasing warm season heavy rain (Allan & Soden, 2008) suggest that the probability of wet season X + n will also increase. In contrast, an increasing probability of dry seasons caused by warmer temperatures and enhanced aridity would likely mean more X + n seasons with soil moisture traces dominated by their own P regime, making high MI content between seasons even less likely than at present. During the 1950s drought in the SWUS, impacted ecosystems exhib-

ited a widespread shift in which high elevation forest ecosystems (ponderosa pine forest) began to resemble lower elevation woodland systems (pinyon-juniper woodlands) (Allen & Breshears, 1998), suggesting a sustained transfer of dry conditions across the region through time. We postulate that this shift likely coincided with increased probability of dry X season MI content with season X + n that could have limited the small positive impact of near-average X + n season P.

6. Conclusions

In this study, we evaluated P-soil moisture (θ) relationships across nine sites comprising three forest and woodland elevation gradients in the southwestern US, with a particular focus on the influence of above- and below-average seasonal P on θ at different depths in the soil profile. Three distinct seasons—a winter season when P was stored above-ground as snow, and moisture infiltration into the soil profile was very low, a spring season that began at the onset of sustained snowmelt infiltration into the soil profile and ended when winter (snowfall) and spring (rainfall) θ inputs were depleted, and a summer season when θ inputs were dependent on rainfall—were shifted in time between high and low elevation sites, with θ at low elevation sites experiencing less influence of winter P, a shorter spring season, and earlier and longer depletion of θ compared to high elevation sites. θ dynamics at shallow soil depths (0–20 cm) were largely decoupled from those at intermediate depths (50 cm), alluding to greater influence of spring and summer rainfall on shallow soil layers, and greater influence of winter snowfall on deeper layers. A high influence of seasonal patterns of θ on those in subsequent seasons was uncommon, but increased substantially in cases where the first season experienced above- or below-average P, and the subsequent season experienced near average P. These results illustrate that the dynamics of diverse forest and woodland sites of the SWUS may be organized across relatively broad elevational categories, and may be elucidated using relatively simple measures of seasonal θ . We propose that understanding future change to forests and woodlands in this region may be sharpened through understanding of seasonal linkages between P and θ , which display common patterns across elevation and depth in the soil.

Appendix A: Correlations Between Comparative Metrics

Tables of correlations between all soil moisture derived metrics at soil depths 0–10 cm (Table A1), 10–20 cm (Table A2), and 50 cm (Table A3).

Table A1
Significant Correlations Between All Comparative Metrics and Elevation at Soil Depth 0–10 cm ($p < 0.05$)

	Max SWE	Max SWE DOY	Si DOY	Si θ	Sp DOY	Sp θ	Sd DOY	St	Σ P input	$D_{>\bar{\theta}}$	$D_{<\bar{\theta}}$	$D_{<20}$	$D_{<10}$	L
Max SWE DOY	–													
Si DOY	–	–												
Si θ	0.33	–	–0.40											
Sp DOY	–	–	0.41	–0.51										
Sp θ	0.43	–	–	0.64	–									
Sd DOY	–	–0.34	–	–	0.54	0.39								
St	–	–0.42	–0.34	–	0.48	0.34	0.89							
Σ P input	–	–	–	0.45	–0.40	–	–0.54	–0.41						
$D_{>\bar{\theta}}$	–	–	–0.41	0.37	–0.31	–	–	0.44	–					
$D_{<\bar{\theta}}$	–	–	–	–	–0.40	–0.47	–0.64	–0.77	–	–				
$D_{<20}$	–	–	–	–0.39	–	–0.43	–	–0.49	–	–	0.60			
$D_{<10}$	–	–	–	–	–	–0.30	–	–0.38	–	–	0.55	0.73		
L	–	0.34	–	–	–0.54	–0.39	1	–0.89	0.54	–	0.64	–	–	
Elevation	–	–	–	–0.57	0.62	–	0.37	–	–0.31	–	–	–0.32	–	–

Note. A dash indicated a nonsignificant relationship and negative signs indicate a negative relationship.

Table A2
Significant Correlations Between All Comparative Metrics and Elevation at Soil Depth 10–20 cm ($p < 0.05$)

	Max SWE	Max SWE DOY	Si DOY	Si θ	Sp DOY	Sp θ	Sd DOY	St	Σ P input	$D_{>\bar{\theta}}$	$D_{<\bar{\theta}}$	$D_{<20}$	$D_{<10}$	L
Max SWE DOY	–													
Si DOY	–	–												
Si θ	0.36	–	–											
Sp DOY	–	–	–	–0.64										
Sp θ	0.51	–	–	0.74	–									
Sd DOY	0.34	–	–	–	0.36	0.53								
St	–	–	–0.56	–	0.60	–	0.90							
Σ P input	–	–	–	–	–	–	–0.35	–						
$D_{>\bar{\theta}}$	–	–	–	0.58	–0.52	0.45	–	–	–					
$D_{<\bar{\theta}}$	–	–	–	–	–	–0.57	–0.55	–0.53	–	–0.70				
$D_{<20}$	–	–	–	–0.56	–	–0.61	–0.36	–	–0.30	–0.53	0.68			
$D_{<10}$	–	–	–	–0.38	–	–0.40	–	–0.34	–	–0.40	0.47	0.87		
L	–0.34	–	–	–	–0.36	–0.53	1	–0.90	0.35	–	0.55	0.36	–	
Elevation	–	–	–	–0.64	0.69	–	0.51	0.46	–	–0.32	–	–	–	–0.51

Note. A dash indicated a nonsignificant relationship and negative signs indicate a negative relationship.

Table A3
Significant Correlations Between All Comparative Metrics and Elevation at Soil Depth 50 cm ($p < 0.05$)

	Max SWE	Max SWE DOY	Si DOY	Si θ	Sp DOY	Sp θ	Sd DOY	St	Σ P input	$D_{>\bar{\theta}}$	$D_{<\bar{\theta}}$	$D_{<20}$	$D_{<10}$	L
Max SWE DOY	–													
Si DOY	–	–												
Si θ	–	–	–											
Sp DOY	–	–	0.59	–										
Sp θ	0.77	–	–0.46	0.54	–									
Sd DOY	–	–	–	–	0.63	–								
St	0.50	–	–0.71	–	–	0.52	0.49							
Σ P input	0.53	0.49	–	–	–	–	–	–						
$D_{>\bar{\theta}}$	0.48	–	–0.51	–	–	0.55	–	0.59	–					
$D_{<\bar{\theta}}$	–	–	–	–	–0.61	–	–0.70	–0.51	–	–0.62				
$D_{<20}$	–0.55	–	–	–	–0.56	–	–0.69	–0.58	–	–0.50	0.87			
$D_{<10}$	–	–	–	–	–	–	–	–	–	–	0.48	0.60		
L	–	–	–	–	–0.63	–	1	–0.49	–	–	0.70	0.69	–	
Elevation	–	–	–	–	–	–	–	–	–	–	–0.46	–	–	–

Note. A dash indicated a nonsignificant relationship and negative signs indicate a negative relationship. Since soil moisture at 50 cm was only measured at NMEG, these relationships apply to that gradient.

Appendix B: Soil Moisture Analyses

Expanded results of soil moisture at deeper layers (Figure B1, expansion on Figure 2); Transfer Entropy (TE) analysis of soil moisture relationships across soil depths (Figure B2, expansion on Figure 6); and Mutual Information content analysis of soil moisture across winter, spring and summer seasons (Figure B3, expansion on Figure 7).

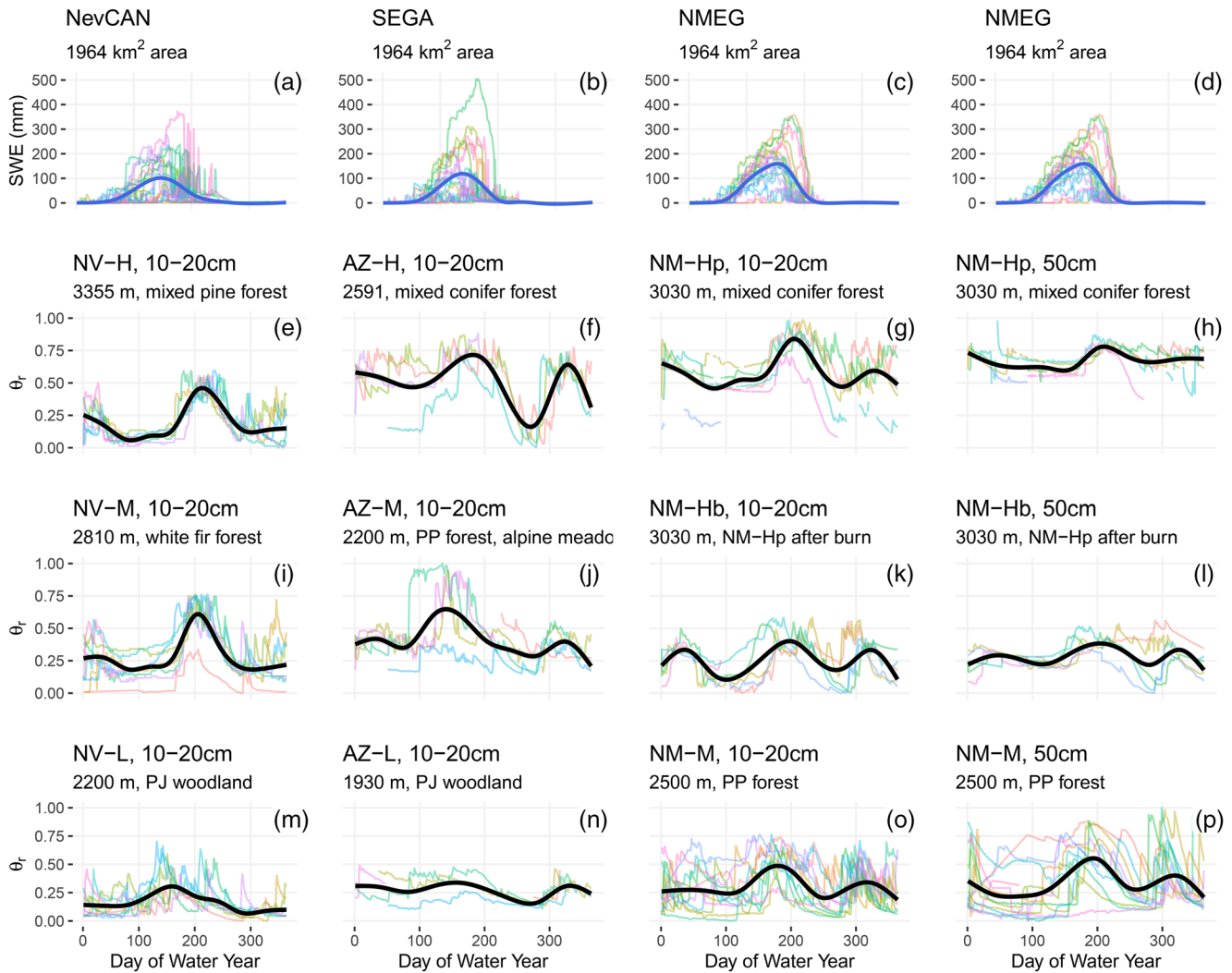


Figure B1. Time series plots of estimated snow water equivalent SWE [mm] for each elevation gradient (a–c), and observed θ_r from 10 to 20 cm (e–g, i–k, and m–o), and 50 cm (h, l, and p) for all sites. Colored lines illustrate θ_r in individual years, and the black lines illustrate a smoothed trend.

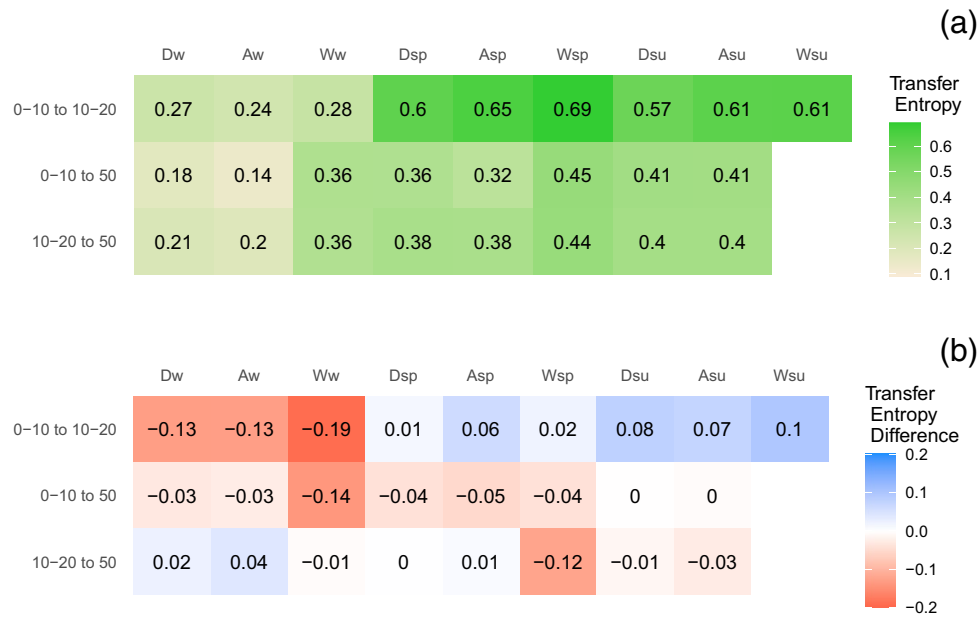


Figure B2. Transfer entropy (TE) values of relative extractable soil moisture [θ_r ; $\text{mm}^3 \text{mm}^{-3}$] for above-average (W), below-average (D), and near average (A) seasonal precipitation totals (w: winter; sp: spring; su: summer) between 0–10, 10–20, and 50 cm soil depths (a), and TE compared between θ -defined seasons and month-defined seasons (θ -defined TE minus month-defined TE; b). In (a), higher TE values indicate greater information transfer between soil layers.

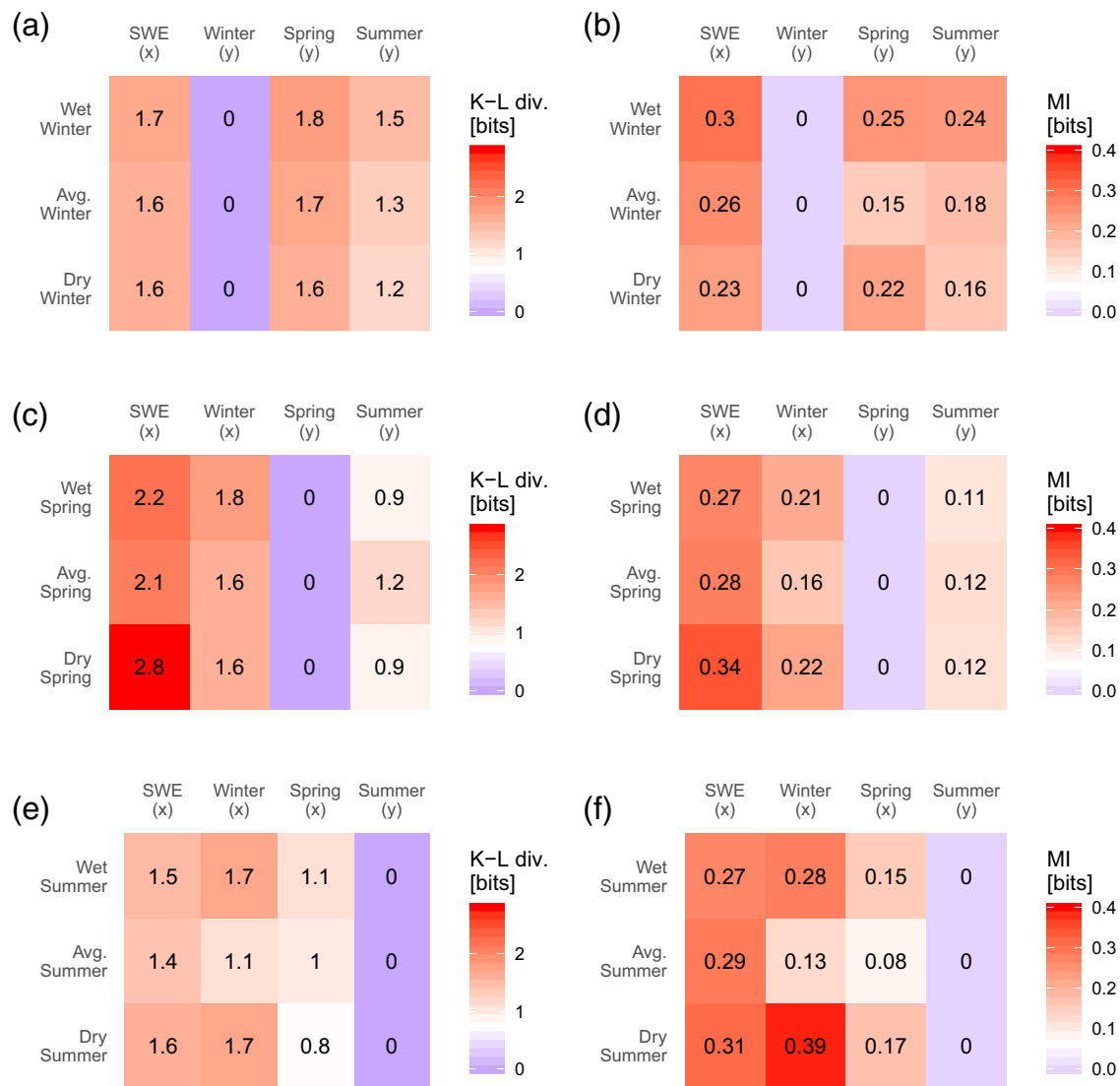


Figure B3. θ predictability by θ -defined season (winter, a and b; spring, c and d; and summer, e and f) under different seasonal P conditions, measured by K-L divergence [K-L] and mutual information [MI]. Each tile represents the mean of all comparisons of θ , distributions of seasons winter (a, b), spring (c, d), and summer (e, f) to the distributions of SWE and winter, spring, and summer θ , by year and site. These comparisons were grouped by wet ($P > +25\%$ site mean), dry ($P < -25\%$ site mean), and average ($P > -25\%$ and $< +25\%$ site mean) seasons and averaged across soil depths. Values are shown as diverging from the mean of each measure, with blue tiles showing relatively higher shared information and red tiles showing relatively low shared information.

Data Availability Statement

Data sets for this research are available in the following repositories: data for sites NM-M (AmeriFlux site US-Vcp), NM-Hp, and NM-Hb (AmeriFlux site US-Vcm) are available through the AmeriFlux Network data portal [<https://doi.org/10.17190/AMF/1246122> and <https://doi.org/10.17190/AMF/1246121> respectively; no access restrictions], data for sites AZ-H (SEGA site Camp Colton), AZ-M (SEGA site Arboretum), and AZ-L (SEGA site Blue Chute) are available through The Southwest Experimental Garden Array data portal [<https://data.sega.nau.edu/segaWeb/index.jsp>; no access restrictions], and climate and soil moisture data for sites NV-H (NevCAN site Snake Range Subalpine west), NV-M (NevCAN site Snake Range Montane west), and NV-L (NevCAN site Snake Range Pinyon-Juniper west) are available through The Nevada Climate-ecohydrological Assessment Network data portal [https://nevcan.dri.edu/data_download.html;noaccessrestrictions].

Acknowledgments

We wish to acknowledge the efforts of the NevCAN team, Brad Lyles, and Greg McCurdy in particular. Their primary contributions to sensor installation and maintenance over time was critical to obtaining a continuous time series of soil moisture, temperature, and precipitation data from the NevCAN stations. We wish to acknowledge funding from DOE through the Ameriflux Management Project and Catalina-Jemez Critical Zone Observatory for NMEG data sets (Ameriflux core sites: US-Vcp, US-Vcm). We thank Troy Wood, Stella Copeland, Austin Rueda, Kaitlyn Toledo, Jessica Hartsell, and Jonathan Paklaian for field assistance. J. B. Bradford was supported by the USGS Ecosystems Mission Area and the North Central Climate Adaptation Science Center. We would like to thank Nathaniel A. Brunzell at the University of Kansas for advice on Information Theory. Any use of trade, firm, or product name is for descriptive purposes only and does not imply endorsement by the U.S. Government.

References

Adams, D. K., & Comrie, A. C. (1997). The North American Monsoon. *Bulletin of the American Meteorological Society*, 78(7), 18. [https://doi.org/10.1175/1520-0477\(1997\)078<2197:tnam>2.0.co;2](https://doi.org/10.1175/1520-0477(1997)078<2197:tnam>2.0.co;2)

Allan, R. P., & Soden, B. J. (2008). Atmospheric warming and the amplification of precipitation extremes. *Science*, 321(5895), 1481–1484. <https://doi.org/10.1126/science.1160787>

Allen, C. D., & Breshears, D. D. (1998). Drought-induced shift of a forest-woodland ecotone: Rapid landscape response to climate variation. *Proceedings of the National Academy of Sciences of the United States of America*, 95(25), 14839–14842. <https://doi.org/10.1073/pnas.95.25.14839>

Anderson-Teixeira, K. J., Delong, J. P., Fox, A. M., Brese, D. A., & Litvak, M. E. (2011). Differential responses of production and respiration to temperature and moisture drive the carbon balance across a climatic gradient in New Mexico. *Global Change Biology*, 17(1), 410–424. <https://doi.org/10.1111/j.1365-2486.2010.02269.x>

Bales, R. C., Hopmans, J. W., O’Geen, A. T., Meadows, M., Hartsough, P. C., Kirchner, P., et al. (2011). Soil moisture response to snowmelt and rainfall in a Sierra Nevada Mixed-conifer forest. *Vadose Zone Journal*, 10(3), 786. <https://doi.org/10.2136/vzj2011.0001>

Behrendt, S., Dimpfl, T., Peter, F. J., & Zimmermann, D. J. (2019). Rtransferentropy – Quantifying information flow between different time series using effective transfer entropy. *SoftwareX*, 10, 100265. <https://doi.org/10.1016/j.softx.2019.100265>

Bell, D. M., Bradford, J. B., & Lauenroth, W. K. (2014). Mountain landscapes offer few opportunities for high-elevation tree species migration. *Global Change Biology*, 20, 1441–1451. <https://doi.org/10.1111/gcb.12504>

Berndt, H. W., & Gibbons, R. D. (1958). *Root distribution of some native trees and understory plants growing on three sites within ponderosa pine watersheds in Colorado* (Technical Report). Fort Collins, CO: U.S. Forest Service. <https://doi.org/10.5962/bhl.title.80878>

Biederman, J. A., Scott, R. L., Arnone, J. A., III, Jasoni, R. L., Litvak, M. E., Moreo, M. T., et al. (2018). Shrubland carbon sink depends upon winter water availability in the warm deserts of North America. *Agricultural and Forest Meteorology*, 249, 407–419. <https://doi.org/10.1016/j.agrformet.2017.11.005>

Blankinship, J. C., Meadows, M. W., Lucas, R. G., & Hart, S. C. (2014). Snowmelt timing alters shallow but not deep soil moisture in the Sierra Nevada. *Water Resources Research*, 50(2), 1448–1456. <https://doi.org/10.1002/2013WR014541>

Bradford, J. B., Schlaepfer, D. R., Lauenroth, W. K., & Palmquist, K. A. (2020). Robust ecological drought projections for drylands in the 21st century. *Global Change Biology*, 26(7), 3906–3919. <https://doi.org/10.1111/gcb.15075>

Breshears, D. D., Cobb, N. S., Rich, P. M., Price, K. P., Allen, C. D., Balice, R. G., et al. (2005). Regional vegetation die-off in response to global-change-type drought. *Proceedings of the National Academy of Sciences of the United States of America*, 102(42), 15144–15148. <https://doi.org/10.1073/pnas.0505734102>

Breshears, D. D., Myers, O. B., Meyer, C. W., Barnes, F. J., Zou, C. B., Allen, C. D., et al. (2009). Tree die-off in response to global change-type drought: mortality insights from a decade of plant water potential measurements. *Frontiers in Ecology and the Environment*, 7, 185–189. <https://doi.org/10.1890/080016>

Brown, P. M., & Wu, R. (2005). Climate and disturbance forcing of episodic tree recruitment in a southwestern ponderosa pine forest. *Ecology*, 86(11), 3030–3038. <https://doi.org/10.1890/05-0034>

Brown-Mitic, C., Shuttleworth, W. J., Chawn Harlow, R., Petti, J., Burke, E., & Bales, R. (2007). Seasonal water dynamics of a sky island subalpine forest in semi-arid southwestern United States. *Journal of Arid Environments*, 69(2), 237–258. <https://doi.org/10.1016/j.jaridenv.2006.09.005>

Cayan, D. R., Das, T., Pierce, D. W., Barnett, T. P., Tyree, M., & Gershunov, A. (2010). Future dryness in the southwest US and the hydrology of the early 21st century drought. *Proceedings of the National Academy of Sciences of the United States of America*, 107(50), 21271–21276. <https://doi.org/10.1073/pnas.0912391107>

Crausbay, S. D., Ramirez, A. R., Carter, S. L., Cross, M. S., Hall, K. R., Bathke, D. J., et al. (2017). Defining ecological drought for the twenty-first century. *Bulletin of the American Meteorological Society*, 98, 2543–2550. <https://doi.org/10.1175/BAMS-D-16-0292.1>

Crimmins, T. M., Crimmins, M. A., & Bertelsen, C. D. (2010). Complex responses to climate drivers in onset of spring flowering across a semi-arid elevation gradient. *Journal of Ecology*, 98(5), 1042–1051. <https://doi.org/10.1111/j.1365-2745.2010.01696.x>

Demaria, E. M. C., Hazenberg, P., Scott, R. L., Meles, M. B., Nichols, M., & Goodrich, D. (2019). Intensification of the North American Monsoon rainfall as observed from a long-term high-density gauge network. *Geophysical Research Letters*, 46(12), 6839–6847. <https://doi.org/10.1029/2019GL082461>

Devitt, D., Bird, B., Lyles, B., Fenstermaker, L., Jasoni, R., Strachan, S., et al. (2018). Assessing near surface hydrologic processes and plant response over a 1600 m mountain valley gradient in the Great Basin, NV, USA. *Water*, 10(4), 420. <https://doi.org/10.3390/w10040420>

Dobrowski, S. Z. (2011). A climatic basis for microrefugia: The influence of terrain on climate. *Global Change Biology*, 17, 1022–1035. <https://doi.org/10.1111/j.1365-2486.2010.02263.x>

Dodson, E. K., & Root, H. T. (2013). Conifer regeneration following stand-replacing wildfire varies along an elevation gradient in a ponderosa pine forest, Oregon, USA. *Forest Ecology and Management*, 302, 163–170. <https://doi.org/10.1016/j.foreco.2013.03.050>

Famiglietti, J. S., Devereaux, J., Laymon, C., Tsegaye, T., Houser, P. R., Jackson, T. J., et al. (1999). Ground-based investigation of soil moisture variability within remote sensing footprints during the Southern Great Plains 1997 (SGP97) Hydrology Experiment. *Water Resources Research*, 35(6), 1839–1851. <https://doi.org/10.1029/1999wr900047>

Fischer, E. M., & Knutti, R. (2016). Observed heavy precipitation increase confirms theory and early models. *Nature Climate Change*, 6(11), 986–991. <https://doi.org/10.1038/nclimate3110>

Hamlet, A. F., Mote, P. W., Clark, M. P., & Lettenmaier, D. P. (2007). Twentieth-century trends in runoff, evapotranspiration, and soil moisture in the western United States. *Journal of Climate*, 20(8), 1468–1486. <https://doi.org/10.1175/jcli4051.1>

Hartsell, J. A., Copeland, S. M., Munson, S. M., Butterfield, B. J., & Bradford, J. B. (2020). Gaps and hotspots in the state of knowledge of pinyon-juniper communities. *Forest Ecology and Management*, 455, 117628. <https://doi.org/10.1016/j.foreco.2019.117628>

Hausser, J., & Strimmer, K. (2009). Entropy inference and the James-Stein estimator, with application to nonlinear gene association networks. *Journal of Machine Learning Research*, 10, 1449–1484.

Hengl, T., de Jesus, J. M., MacMillan, R. A., Batjes, N. H., Heuvelink, G. B. M., Ribeiro, E., et al. (2014). Soilgrids1km – Global soil information based on automated mapping. *PLoS One*, 9(8), 1–17. <https://doi.org/10.1371/journal.pone.0105992>

Herrmann, S. M., Didan, K., Barreto-Munoz, A., & Crimmins, M. A. (2016). Divergent responses of vegetation cover in Southwestern US ecosystems to dry and wet years at different elevations. *Environmental Research Letters*, 11(12), 124005. <https://doi.org/10.1088/1748-9326/11/12/124005>

- Hunsaker, C. T., Whitaker, T. W., & Bales, R. C. (2012). Snowmelt runoff and water yield along elevation and temperature gradients in California's southern Sierra Nevada. *Journal of the American Water Resources Association*, 48(4), 667–678. <https://doi.org/10.1111/j.1752-1688.2012.00641.x>
- Hupet, F., & Vanlooster, M. (2002). Intraseasonal dynamics of soil moisture variability within a small agricultural maize cropped field. *Journal of Hydrology*, 261(1–4), 86–101. [https://doi.org/10.1016/S0022-1694\(02\)00016-1](https://doi.org/10.1016/S0022-1694(02)00016-1)
- Hurteau, M. D., Bradford, J. B., Fulé, P. Z., Taylor, A. H., & Martin, K. L. (2014). Climate change, fire management, and ecological services in the southwestern US. *Forest Ecology and Management*, 327, 280–289. <https://doi.org/10.1016/j.foreco.2013.08.007>
- Jones, S. M., & Gutzler, D. S. (2016). Spatial and seasonal variations in aridification across Southwest North America. *Journal of Climate*, 29(12), 4637–4649. <https://doi.org/10.1175/JCLI-D-14-00852.1>
- Kerhoulas, L. P., Kolb, T. E., & Koch, G. W. (2013). Tree size, stand density, and the source of water used across seasons by ponderosa pine in northern Arizona. *Forest Ecology and Management*, 289, 425–433. <https://doi.org/10.1016/j.foreco.2012.10.036>
- Knowles, J. F., Molotch, N. P., Trujillo, E., & Litvak, M. E. (2018). Snowmelt-driven trade-offs between early and late season productivity negatively impact forest carbon uptake during drought. *Geophysical Research Letters*, 45(7), 3087–3096. <https://doi.org/10.1002/2017gl076504>
- Koepke, D. F., Kolb, T. E., & Adams, H. D. (2010). Variation in woody plant mortality and dieback from severe drought among soils, plant groups, and species within a northern Arizona ecotone. *Oecologia*, 163(4), 1079–1090. <https://doi.org/10.1007/s00442-010-1671-8>
- Kolb, T., Dore, S., & Montes-Helu, M. (2013). Extreme late-summer drought causes neutral annual carbon balance in southwestern ponderosa pine forests and grasslands. *Environmental Research Letters*, 8(1), 015015. <https://doi.org/10.1088/1748-9326/8/1/015015>
- Limousin, J.-M., Bickford, C. P., Dickman, L. T., Pangle, R. E., Hudson, P. J., Boutz, A. L., et al. (2013). Regulation and acclimation of leaf gas exchange in a piñon-juniper woodland exposed to three different precipitation regimes. *Plant, Cell and Environment*, 36(10), 1812–1825. <https://doi.org/10.1111/pce.12089>
- Littell, J. S., McKenzie, D., Peterson, D. L., & Westerling, A. L. (2009). Climate and wildfire area burned in western U.S. ecoprovinces, 1916–2003. *Ecological Applications*, 19(4), 1003–1021. <https://doi.org/10.1890/07-1183.1>
- Loik, M. E., Breshears, D. D., Lauenroth, W. K., & Belnap, J. (2004). A multi-scale perspective of water pulses in dryland ecosystems: Climatology and ecohydrology of the western USA. *Oecologia*, 141(2), 269–281. <https://doi.org/10.1007/s00442-004-1570-y>
- Ma, S., Baldocchi, D. D., Xu, L., & Hehn, T. (2007). Inter-annual variability in carbon dioxide exchange of an oak/grass savanna and open grassland in California. *Agricultural and Forest Meteorology*, 147(3–4), 157–171. <https://doi.org/10.1016/j.agrformet.2007.07.008>
- McNamara, J. P., Chandler, D., Seyfried, M., & Achet, S. (2005). Soil moisture states, lateral flow, and streamflow generation in a semi-arid, snowmelt-driven catchment. *Hydrological Processes*, 19(20), 4023–4038. <https://doi.org/10.1002/hyp.5869>
- National Operational Hydrologic Remote Sensing Center. (2004). *Snow Data Assimilation System (SNODAS) Data Products at NSDIC, Version 1*. (Masked data from Oct 2003 to Oct 2019). Boulder, CO: NSIDC: National Snow and Ice Data Center. <https://doi.org/10.7265/N5TB14TC>
- Newman, B. D., Campbell, A. R., & Wilcox, B. P. (1997). Tracer-based studies of soil water movement in semi-arid forests of New Mexico. *Journal of Hydrology*, 196(1–4), 251–270. [https://doi.org/10.1016/S0022-1694\(96\)03320-3](https://doi.org/10.1016/S0022-1694(96)03320-3)
- Notaro, M., Liu, Z., Gallimore, R. G., Williams, J. W., Gutzler, D. S., & Collins, S. (2010). Complex seasonal cycle of ecohydrology in the Southwest United States. *Journal of Geophysical Research*, 115, G04034. <https://doi.org/10.1029/2010JG001382>
- Oldfather, M. F., Britton, M. N., Papper, P. D., Koontz, M. J., Halbur, M. M., Dodge, C., et al. (2016). Effects of topoclimatic complexity on the composition of woody plant communities. *AoB PLANTS*, 8, plw049. <https://doi.org/10.1093/aobpla/plw049>
- Pérez-Cruz, F. (2008). *Kullback-Leibler divergence estimation of continuous distributions*. 2008 IEEE International Symposium on Information Theory (pp. 1666–1670). <https://doi.org/10.1109/isit.2008.4595271>
- Petrie, M. D., Bradford, J. B., Hubbard, R. M., Lauenroth, W. K., Andrews, C. M., & Schlaepfer, D. R. (2017). Climate change may restrict dryland forest regeneration in the 21st century. *Ecology*, 98(6), 1548–1559. <https://doi.org/10.1002/ecy.1791>
- Petrie, M. D., Collins, S. L., Gutzler, D. S., & Moore, D. M. (2014). Regional trends and local variability in monsoon precipitation in the northern Chihuahuan Desert, USA. *Journal of Arid Environments*, 103, 63–70. <https://doi.org/10.1016/j.jaridenv.2014.01.005>
- Petrie, M. D., Pockman, W. T., Pangle, R. E., Limousin, J. M., Plaut, J. A., & McDowell, N. G. (2015). Winter climate change promotes altered spring growing season in piñon pine-juniper woodlands. *Agricultural and Forest Meteorology*, 214–215, 357–368. <https://doi.org/10.1016/j.agrformet.2015.08.269>
- PRISM Climate Group at Oregon State University. (2004). *Prism time series data*. Retrieved from <http://prism.oregonstate.edu>
- R Core Team. (2019). *R: A language and environment for statistical computing [Computer software manual]*. Vienna, Austria. Retrieved from <https://www.R-project.org/>
- Rocca, M. E., Brown, P. M., MacDonald, L. H., & Carrico, C. M. (2014). Climate change impacts on fire regimes and key ecosystem services in rocky mountain forests. *Forest Ecology and Management*, 327, 290–305. <https://doi.org/10.1016/j.foreco.2014.04.005>
- Saxton, K. E., & Rawls, W. J. (2006). Soil water characteristic estimates by texture and organic matter for hydrologic solutions. *Soil Science Society of America Journal*, 70(5), 1569–1578. <https://doi.org/10.2136/sssaj2005.0117>
- Schlaepfer, D. R., Lauenroth, W. K., & Bradford, J. B. (2012). Consequences of declining snow accumulation for water balance of mid-latitude dry regions. *Global Change Biology*, 18, 1988–1997. <https://doi.org/10.1111/j.1365-2486.2012.02642.x>
- Schwinning, S., Litvak, M. E., Pockman, W., Pangle, R., Fox, A. M., Huang, C.-W., & McIntire, C. (2020). A 3-dimensional model of *Pinus edulis* and *Juniperus monosperma* root distributions in New Mexico: Implications for soil water dynamics. *Plant and Soil*, 450, 337–355. <https://doi.org/10.1007/s11104-020-04446-y>
- Seager, R., & Vecchi, G. A. (2010). Greenhouse warming and the 21st century hydroclimate of southwestern North America. *Proceedings of the National Academy of Sciences of the United States of America*, 107(50), 21277–21282. <https://doi.org/10.1073/pnas.0910856107>
- Strachan, S. (2016). Precipitation and conifer response in semiarid mountains: A case from the 2012–15 drought in the Great Basin, USA. In G. B. Greenwood & J. F. Shroder (Eds.), *Mountain ice and water: Investigations of the hydrologic cycle in alpine environments* (Vol. 21, pp. 193–238). Elsevier. <https://doi.org/10.1016/B978-0-444-63787-1.00005-6>
- Swetnam, T. W., & Betancourt, J. L. (1998). Mesoscale disturbance and ecological response to decadal climatic variability in the American Southwest. *Journal of Climate*, 11(20), 3128–3147.
- Thomas, C. K., Law, B. E., Irvine, J., Martin, J. G., Pettijohn, J. C., & Davis, K. J. (2009). Seasonal hydrology explains interannual and seasonal variation in carbon and water exchange in a semiarid mature ponderosa pine forest in central Oregon. *Journal of Geophysical Research*, 114, G04006. <https://doi.org/10.1029/2009JG001010>
- Van Loon, A. F., Tjeldeman, E., Wanders, N., Van Lanen, H. A., Teuling, A. J., & Uijlenhoet, R. (2014). How climate seasonality modifies drought duration and deficit. *Journal of Geophysical Research: Atmospheres*, 119(8), 4640–4656. <https://doi.org/10.1002/2013JD020383>
- Van Loon, A. F., & Van Lanen, H. A. J. (2012). A process-based typology of hydrological drought. *Hydrology and Earth System Sciences*, 16(7), 1915–1946. <https://doi.org/10.5194/hess-16-1915-2012>

- West, A. G., Hultine, K. R., Burtch, K. G., & Ehleringer, J. R. (2007). Seasonal variations in moisture use in a piñon–juniper woodland. *Oecologia*, *153*(4), 787–798. <https://doi.org/10.1007/s00442-007-0777-0>
- Whittaker, R. H., & Niering, W. A. (1965). Vegetation of the Santa Catalina Mountains, Arizona: A gradient analysis of the south slope. *Ecology*, *46*(4), 429–452. <https://doi.org/10.2307/1934875>
- Williams, A. P., Allen, C. D., Macalady, A. K., Griffin, D., Woodhouse, C. A., Meko, D. M., et al. (2013). Temperature as a potent driver of regional forest drought stress and tree mortality. *Nature Climate Change*, *3*(3), 292–297. <https://doi.org/10.1038/nclimate1693>
- Williams, A. P., Allen, C. D., Millar, C. I., Swetnam, T. W., Michaelsen, J., Still, C. J., & Leavitt, S. W. (2010). Forest responses to increasing aridity and warmth in the southwestern United States. *Proceedings of the National Academy of Sciences of the United States of America*, *107*(50), 21289–21294. <https://doi.org/10.1073/pnas.0914211107>
- Williams, C. J., McNamara, J. P., & Chandler, D. G. (2009). Controls on the temporal and spatial variability of soil moisture in a mountainous landscape: The signature of snow and complex terrain. *Hydrology and Earth System Sciences*, *13*(7), 1325–1336. <https://doi.org/10.5194/hess-13-1325-2009>
- Young, J. A., & Budy, J. D. (1979). Historical use of Nevada's pinyon-juniper woodlands. *Forest and Conservation History*, *23*(3), 112–121. <https://doi.org/10.2307/4004663>
- Zhang, J., Ritchie, M., Maguire, D., & Oliver, W. (2013). Thinning ponderosa pine (*Pinus ponderosa*) stands reduces mortality while maintaining stand productivity. *Canadian Journal of Forest Research*, *43*, 311–320. <https://doi.org/10.1139/cjfr-2012-0411>
- Zlotin, R., & Parmenter, R. (2008). Patterns of mast production in pinyon and juniper woodlands along a precipitation gradient in central New Mexico (Sevilleta National Wildlife Refuge). *Journal of Arid Environments*, *72*(9), 1562–1572. <https://doi.org/10.1016/j.jaridenv.2008.02.021>